RM No. L7E23
Copy No. 173

NACA RM No. L7E23

NACA

RESEARCH MEMORANDUM

LOW-SPEED CHARACTERISTICS IN PITCH OF A 42° SWEPTBACK WING WITH ASPECT RATIO 3.9 AND CIRCULAR-ARC AIRFOIL SECTIONS

By

Robert H. Neely and William Koven

Langley Memorial Aeronautical Laboratory
Langley Field, Va.

NATIONAL ADVISORY COMMITTEE
FOR AERONAUTICS

WASHINGTON
November 13, 1947

NATIONAL ADVISORY COMMITTEE FOR AERONAUTICS

RESEARCH MEMORANDUM

LOW-SPEED CHARACTERISTICS IN PITCH OF A 42° SWEPTBACK WING WITH ASPECT RATIO 3.9 AND CIRCULAR-ARC AIRFOIL SECTIONS

By Robert H. Neely and William Koven

SUMMARY

Results are presented of tests made in the Langley 19-foot pressure tunnel to determine the low-speed pitch characteristics of a 42° sweptback wing with circular-arc airfoil sections, an aspect ratio of 3.9, and a taper ratio of 0.625. The effects on the wing characteristics of extensible round-nose leading-edge flaps located on the outboard 70 percent of the semispan, and of a fuselage with fineness ratio 10.2 located in low, middle, and high positions were investigated. The tests covered a range of Reynolds number from 3.09×10^6 to 9.60×10^6.

The characteristics of the basic wing from low-speed considerations were poor. Maximum lift coefficients of about 0.85 and 0.95 were obtained for the plain wing and for the wing with half-span split flaps deflected 60°, respectively. Large unstable variations in pitching moment caused by tip stalling and appreciable increases in drag occurred at moderate angles of attack. The wing with leading-edge flaps exhibited reasonably good characteristics. The addition of leading-edge flaps increased $C_{L_{max}}$ to 1.18 for the wing without split flaps and to 1.52 for the wing with split flaps and eliminated the large unstable variations in pitching moment by delaying stalling over the outboard sections of the wing. The fuselage in any of the three positions produced no large effects on the characteristics of the basic wing. For the wing with leading-edge flaps the pitching-moment variation near maximum lift was reversed from a stable to an unstable condition by the addition of the fuselage in the middle position. Over the range of Reynolds number tested, there was no appreciable scale effect on the characteristics of the wing.

A comparison of the basic wing characteristics with those of an NACA 64_1-112 sweptback wing with nearly identical plan form revealed that, from low-speed considerations, the basic circular-arc wing was decidedly inferior in most respects to the 64-series wing. With leading-edge flaps the characteristics of the two

wings more nearly approached each other, although the drag of the circular-arc wing was still considerably higher than that of the 64-series wing.

INTRODUCTION

The use of sharp leading-edge airfoil sections on swept wings has been contemplated as a means of reducing drag at supersonic velocities. Inasmuch as adverse longitudinal stability and stalling characteristics on swept wings with conventional profiles have been encountered at low speed in previous investigations, it was considered desirable to investigate the low-speed characteristics of a swept wing with a sharp leading edge. A series of tests were made, therefore, in the Langley 19-foot pressure tunnel on a wing having 42° sweepback at the leading edge and incorporating thin symmetrical circular-arc airfoil sections. The wing had an aspect ratio of 3.9 and a taper ratio of 0.625.

The characteristics of the basic wing in pitch with and without 50-percent semispan split flaps were obtained from force measurements and stall studies over a range of Reynolds number from 3.09×10^6 to 9.60×10^6. To investigate the possibilities of improving the characteristics of the wing by means of a leading-edge device, two types of leading-edge flaps, a flat and a curved flap, of approximately 70-percent span were tested. The effects of a fuselage in several vertical positions on the characteristics of the wing were also determined. As an aid in evaluating the results of this investigation, the data are compared with the results of tests of a wing with nearly identical plan form but incorporating NACA 64_1-112 airfoil sections (references 1 and 2).

COEFFICIENTS AND SYMBOLS

The data are referred to a set of axes coinciding with the wind axes. All coefficients are based upon the dimensions of the basic wing. Pitching moments are computed about the quarter chord of the mean aerodynamic chord.

C_L	lift coefficient (L/qS)
$C_{L_{max}}$	maximum lift coefficient
C_D	drag coefficient (D/qS)

C_m pitching-moment coefficient $(M/qS\bar{c})$

R Reynolds number $(\rho V\bar{c}/\mu)$

M_o Mach number (V/a)

α angle of attack of wing chord line

$\frac{dC_m}{dC_L}$ rate of change of pitching moment with lift coefficient

where

L lift

D drag

M pitching moment about quarter chord of mean aerodynamic chord

S wing area

$\bar{c}$ mean aerodynamic chord measured parallel to the plane of symmetry $\left(\frac{2}{S}\int_0^{b/2} c^2 dy\right)$

$\bar{x}$ distance from the leading edge of the chord at plane of symmetry to quarter-chord point of the mean aerodynamic chord $\left(\frac{2}{S}\int_0^{b/2} cx\ dy\right)$

x longitudinal distance, parallel to plane of symmetry, from the leading edge of the root chord to quarter-chord point of each section

c local chord measured parallel to the plane of symmetry

y spanwise coordinate

b	span
q	free-stream dynamic pressure $\left(\frac{1}{2}\rho V^2\right)$
V	free-stream velocity
ρ	mass density of air
μ	coefficient of viscosity
a	velocity of sound

MODEL

A sketch of the wing and fuselage is presented in figure 1 and a photograph of the wing is shown in figure 2. The wing had an aspect ratio of 3.94 and a ratio of tip chord to root chord of 0.625. A straight line connecting the leading edge of the root and theoretical tip chords was swept back 42.05°. The wing, which was of solid steel construction, was fabricated with a constant radius of 83.26 inches at each spanwise section in a plane perpendicular to the line of maximum thickness indicated in figure 1. Consequently, the leading and trailing edges were slightly curved, the maximum deviation from a straight line joining the leading edges of the root and tip chords being about 0.4 inch. The airfoil sections normal to the line of maximum thickness were symmetrical circular-arc sections having a maximum thickness at 50 percent chord of 10 percent at the root and 6.4 percent at the tip. (See fig. 1.) Parallel to the plane of symmetry, the wing had a thickness of 7.9 percent chord at the root and 5.2 percent chord at the tip. The wing was lacquered and sanded to obtain a smooth surface.

The fuselage was circular in cross section and had a fineness ratio of 10.2. The maximum diameter was 40 percent of the root chord. The center section had removable blocks to permit attachment to the wing at three vertical positions. (See fig. 1.) Ordinates for the fuselage are presented in table I. The fuselage was constructed of laminated mahogany and had a smooth finish.

The model was provided with 20-percent-chord trailing-edge split flaps which were deflected 60° from the lower surface of the wing in a plane normal to the 80-percent (hinge) chord line. (See fig. 3.) For most of the wing-alone tests, these flaps extended over the inboard 50 percent of the wing semispan, but for the wing-fuselage tests and for several wing-alone tests a section of each flap (12.4 percent of the wing semispan) was removed at the center portion of the wing.

These two split-flap configurations are hereinafter referred to as continuous and cut-out split flaps.

Two types of leading-edge flaps were tested; one was flat in cross section and the other, curved. A schematic drawing giving pertinent dimensions is presented in figure 3 and a photograph of the leading-edge flap installations is given in figure 4. The flaps were of constant chord and extended from the 28-percent to the 97.5-percent-semispan station. The flaps were approximately 12 percent chord and 18 percent chord at the inboard and outboard ends, respectively, and were deflected 37° down from the wing chord line in a plane perpendicular to a line joining the leading edges of the root and tip chords. The area of the leading-edge flaps was approximately 10 percent of the wing area. A nose radius was obtained by welding a $\frac{1}{2}$-inch steel tube to the steel flap and then fairing to give a smooth contour.

TESTS

Tests were made in the Langley 19-foot pressure tunnel with the air compressed to 33 pounds per square inch absolute. The wing was supported as shown in figure 2. Lift, drag, and pitching moment were measured for the following values of Reynolds number and Mach number:

R	M_o
3.09×10^6	0.068
5.32	.114
8.20	.179
9.60	.215

The majority of the tests were conducted at Reynolds numbers of 3.09×10^6 and 8.20×10^6. Some wing-alone tests were run at a Reynolds number of 9.60×10^6 and the combination of midwing fuselage and flat-leading-edge flap was tested at a Reynolds number of 5.32×10^6. The stall characteristics of most of the configurations were studied at a Reynolds number of 8.20×10^6, but the flat-leading-edge flap configurations were investigated at a Reynolds number of 5.32×10^6. The stall studies were made by visual observation and from motion-picture records of the behavior of wool tufts attached to the upper surface of the wing at the 10-, 20-, 40-, 60-, 80-, and 90-percent-chord stations.

CORRECTIONS TO DATA

The data presented herein have been corrected for support tare and interference effects and for air-stream misalinement. The jet-boundary corrections to the angle of attack and drag coefficient were calculated from reference 3 and are as follows:

$$\Delta\alpha = 1.00\ C_L$$

$$\Delta C_D = 0.0152\ C_L^2$$

The correction to the pitching-moment coefficient due to the tunnel-induced distortion of the wing loading is

$$\Delta C_m = 0.004\ C_L$$

All corrections were added to the data.

RESULTS AND DISCUSSION

The results of the investigation of the plain wing and the wing with split flaps (hereinafter referred to as basic wing configurations) are presented in figures 5 and 6. These data are compared in figure 7 with data on the NACA 64-series wing of reference 1. The data for the leading-edge-flap tests are given in figures 8 to 11, and the results of the wing-fuselage investigation are presented in figures 12 to 14. To assist in interpreting the lift-drag variations in terms of power-off gliding characteristics, contours of constant gliding speed and constant vertical (sinking) speed are superimposed on the lift-drag polars of several configurations in figure 15. For the constant speed contours a wing loading of 40 pounds per square foot was assumed. The effects of the leading-edge flaps and the fuselage on the longitudinal-stability parameter $\frac{dC_m}{dC_L}$ are shown in figures 16 and 17. A brief summary of some of the important characteristics of the wing in various configurations is presented in table II.

The effects of Reynolds number on the characteristics of the wing were small over the range investigated. For this reason data showing the effect of Reynolds number are given only for the basic wing configuration.

Characteristics of Basic Wing

Stalling characteristics.- The results of the stall studies are presented in figure 5. For the flaps-off configuration the flow assumed a spanwise direction towards the tip near the leading edge of the wing at low lift coefficients. The region of outflow gradually increased, both spanwise and chordwise, until at $C_L \approx 0.5$ stalling began at the leading edge of the wing tip. The stall then progressed slowly inward and rearward as the angle of attack was increased.

The stall pattern for the wing with split flaps was similar to that for the plain wing except that the stalling at the tip began at a higher lift coefficient and extended over a larger portion of the chord.

Force characteristics.- Data given in figure 6 for Reynolds numbers of 3.09×10^6 and 9.60×10^6 show that no appreciable scale effects in this Reynolds number range were evidenced for the wing with either the split flaps off or on. At moderate to high angles of attack the pitching moment was slightly more positive for the higher Reynolds number condition. For the plain wing the increase in Reynolds number caused a reduction in $C_{L_{max}}$ of about 0.04.

The wing exhibited decidedly nonlinear lift characteristics. For the wing without flaps the lift-curve slope increased from a value of 0.055 at zero lift to a value of 0.066 at $C_L = 0.55$ and then decreased as the angle of attack was increased. The low lift-curve slope of this wing at low angles of attack is attributed, to a large degree, to the low aspect ratio of the wing, inasmuch as the lift-curve slope calculated from two-dimensional data for a corresponding unswept wing of the same aspect ratio is within 10 percent of the observed slope. The maximum lift coefficients were about 0.85 for the plain wing and 0.95 for the wing with split flaps. It is of interest to note that the maximum lift coefficient for the plain wing was higher by approximately 0.15 than that obtained in two-dimensional tests of a similar profile (reference 4).

The pitching-moment curves of the wing (fig. 6) were also nonlinear and the variation of the longitudinal-stability parameter $\left(\frac{dC_m}{dC_L}\right)_{\bar{c}/4}$ with lift coefficient was large (fig. 16). In the case of

the plain wing, at zero lift the slope of the pitching-moment curve was positive and at $C_L \approx 0.20$ to 0.50 the wing became neutrally stable or slightly stable. A large unstable variation of the pitching moment occurred between $C_L \approx 0.50$ and $C_{L_{max}}$, and at $C_{L_{max}}$ a stable variation was obtained. The pitching-moment variation for the flapped wing was similar to that of the plain wing. Examination of the stall studies (fig. 5) associates the onset of the destabilizing effect with a rough and stalled region at the wing tips.

The drag coefficients were very high at moderate to high lift coefficients. At equal values of lift coefficient above 0.6 the drag of the wing with flaps was lower than that of the plain wing. It should be pointed out that initial stalling began at a considerably higher lift coefficient for the wing with split flaps as compared with the plain wing, and consequently the large increases in drag occurred later. From figure 15 it may be seen that, for the assumed conditions, the calculated sinking speed is high at all forward speeds for both the plain wing and wing with split flaps.

Comparison with 64-series wing.- A comparison between the characteristics of the wing described herein and a wing of nearly identical plan form but incorporating NACA 64_1-112 airfoil sections (reference 1) is presented in figure 7. The results show that the aerodynamic characteristics of the two wings differ greatly in several important respects notwithstanding the near identity in plan form and that the characteristics of the circular-arc wing are much inferior to those of the NACA 64_1-112 wing.

The data show that much higher maximum lift coefficients and considerably lower drag coefficients were realized for the 64-series wing. The flap effectiveness at $C_{L_{max}}$ was also much greater. For the 64-series wing no large changes in stability occurred up to maximum lift, and at maximum lift the pitching moment broke in an unstable direction. On the other hand, fairly large changes in stability through the lift range and a stable variation in the pitching moment at high angles of attack were noted for the circular-arc wing. The linear character of the lift and pitching-moment curves up to $C_{L_{max}}$ for the 64-series wing indicates a different stall progression from that experienced by the wing with circular-arc sections. For the latter wing, stalling began at a relatively low lift coefficient at the leading edge of the wing tips and gradually spread rearward and inboard; stalling in the case of the 64-series wing (reference 1) occurred suddenly near $C_{L_{max}}$ and encompassed the entire outer half of the wing.

Leading-Edge Flap Investigation

The force and stalling characteristics of the wing were improved by addition of leading-edge flaps to such an extent that reasonably good characteristics were obtained. The effects on the characteristics were nearly the same for either flat flaps or curved flaps.

Force characteristics.- The effect of the leading-edge flaps was to delay separation of the flow to a higher angle of attack. The lift curve, accordingly, was extended until a maximum lift coefficient of approximately 1.18 for the wing without split flaps was attained (fig. 8); the shape of the lift curve near maximum lift was very similar to that of the wing without leading-edge flaps. The maximum lift coefficient with split flaps was about 1.52 (fig. 9), but the lift curve broke more sharply at $C_{L_{max}}$ than was the case without leading-edge flaps.

The addition of leading-edge flaps reduced the drag coefficient at lift coefficients above 0.4 and 0.65 for the plain wing and wing with split flaps, respectively, however, the drag coefficients of the wing with leading-edge flaps were still high in the region of maximum lift. In terms of airplane gliding characteristics (fig. 15) the leading-edge flaps, besides reducing the gliding speed considerably, reduced the sinking speeds at lift coefficients corresponding to the approach condition. The values of sinking speed obtained with leading-edge flap are, for the assumed conditions, in excess of the maximum value of 25 feet per second recommended in reference 5.

The main effects of the leading-edge flaps on the pitching-moment characteristics were the elimination of the large decrease in stability at moderate to high angles of attack that occurred with the basic wing, and a reduction in stability in the low lift coefficient range. The variations of $\left(\frac{dC_m}{dC_L}\right)_{\bar{c}/4}$ with C_L for the wing with and without leading-edge flaps (fig. 16) give some idea of the magnitude of these changes in stability. Above $C_{L_{max}}$ the pitching moment of the wing with leading-edge flaps varied in a stable direction.

The characteristics of the circular-arc wing with leading-edge flaps were quite similar to those of the 64_1-112 wing in a similar configuration (reference 2) with respect to $C_{L_{max}}$ and with respect to the variation of pitching-moment coefficient with lift coefficient at high angles of attack. (See fig. 10.) The drag coefficients of

the circular-arc wing, however, were considerably greater than those of the 64_1-112 wing.

Stalling characteristics.- In contrast to the early tip stalling of the basic wing, stalling of the wing with leading-edge flaps occurred initially in the region near the root (fig. 11), so that no loss in stability occurred throughout the lift range. At moderate lift coefficients rough flow originated behind the inboard end of the leading-edge flap. As the angle of attack was increased, the rough flow spread both inboard and outboard, while the portion of the wing directly behind the inboard end of the flap became stalled. The stalled area then broadened, moving inboard at a faster rate than it progressed outboard. At maximum lift the center section of the wing was almost completely stalled. When the split flaps and flat leading-edge flaps were on (fig. 11(b)), the tips of the wing stalled at approximately the same time as the root sections causing a sudden loss in lift after $C_{L_{max}}$ was reached. For the same condition with curved leading-edge flaps on, tip stalling was not obtained and the stall progression was similar to that shown in figure 11(a).

Effects of Fuselage

Basic wing.- As shown in figure 12, the addition of the fuselage in any of the three vertical positions to the plain wing caused no large changes in the wing characteristics. A slight increase in $C_{L_{max}}$ was obtained with the high and midwing arrangements. The increment in drag at zero lift was about 0.0050 and then decreased at higher lifts. As normally would be expected the fuselage produced a reasonable destabilizing effect throughout the lift range. (See fig. 17.)

For the wing with cut-out split flaps (fig. 13) the addition of the fuselage, as in the case of the plain wing, did not produce any unusually large changes in the characteristics of the wing. It is evident, however, that the high-wing and midwing arrangements had better lift and drag characteristics than either the low-wing arrangement or the fuselage-off condition. Inasmuch as the center section of the flaps was removed for these tests, the increase in lift and reduction in drag experienced when the fuselage was in the high and midwing positions may result from alleviation of the depression of the span loading caused by the flap cut-out. In fact, the characteristics for these two arrangements approach those of the fuselage-off arrangement with the flaps continuing into the root section (fig. 9).

Wing with leading-edge flaps.- The characteristics of the midwing-fuselage combination with flat leading-edge flaps differed in several important respects from those of the wing without the fuselage. (See fig. 14.) The maximum lift coefficient with split flaps off was increased from 1.19 without the fuselage to 1.40 with the fuselage whereas for the wing with split flaps there was little change. The reason for this large difference in fuselage effects on the maximum lift coefficient of the wing with and without split flaps is not clear, and insufficient data are available to analyze fully the effects. The drag coefficients, with split flaps on and off, were noticeably reduced by the addition of the fuselage. At very high angles of attack an unstable pitching moment occurred with the fuselage on, in contrast to the stable moment obtained without the fuselage. The reason for this change in pitching moment at high angles of attack can best be explained by reference to the stall studies presented on figure 11. It is apparent that the fuselage prevented the stall from enveloping the root sections until finally the wing tips commenced to stall; the tip stall produced the unstable pitching moment previously mentioned.

It should be pointed out that data on the NACA 64_1-112 wing in reference 2 suggest the possibility that the aforementioned unstable pitching-moment variation at the stall might be eliminated by either a change in fuselage position or a reduction in the span of the leading-edge flap.

CONCLUSIONS

From the results of the investigation in the Langley 19-foot pressure tunnel of a 42° sweptback wing with thin symmetrical circular-arc airfoil sections, the following conclusions may be drawn:

1. The characteristics of the basic wing, from low-speed considerations, were poor.

2. Maximum lift coefficients of about 0.85 and 0.95 were obtained for the plain wing and for the wing with half-span split flaps, respectively. Large unstable variations in pitching moment caused by tip stalling and appreciable increases in drag occurred at moderate angles of attack.

3. The wing with leading-edge flaps exhibited reasonably good characteristics. The addition of leading-edge flaps increased $C_{L_{max}}$ to 1.18 for the wing without split flaps and to 1.52 for the wing with split flaps and eliminated the large unstable variations in pitching moment by delaying stalling over the outboard sections of the wing.

4. A fuselage located in the low-wing, midwing, and high-wing positions produced no large effects on the characteristics of the basic wing. For the wing with leading-edge flaps the variation of the pitching moment near maximum lift was reversed from a stable to an unstable condition by the addition of the fuselage in the middle position.

5. A variation of Reynolds number from 3.09×10^6 to 9.60×10^6 had no appreciable effect on the characteristics of the wing.

6. A comparison of the basic wing characteristics with those of a 64_1-112 sweptback wing with nearly identical plan form revealed that, from low-speed considerations, the circular-arc wing was decidedly inferior in most respects to the 64-series wing. With leading-edge flaps the characteristics of the two wings more nearly approached each other, although the drag of the circular-arc wing was still considerably higher than that of the 64-series wing.

Langley Memorial Aeronautical Laboratory
National Advisory Committee for Aeronautics
Langley Field, Va.

REFERENCES

1. Neely, Robert H., and Conner, D. William: Aerodynamic Characteristics of a 42° Swept-Back Wing with Aspect Ratio 4 and NACA 64_1-112 Airfoil Sections at Reynolds Numbers from 1,700,000 to 9,500,000. NACA RM No. L7D14, 1947.

2. Graham, Robert R., and Conner, D. William: Investigation of High-Lift and Stall-Control Devices on an NACA 64-Series 42° Swept-back Wing with and without Fuselage. NACA RM No. L7G09, 1947.

3. Eisenstadt, Bertram J.: Boundary-Induced Upwash for Yawed and Swept-Back Wings in Closed Circular Wind Tunnels. NACA TN No. 1265, 1947.

4. Underwood, William J., and Nuber, Robert J.: Two-Dimensional Wind-Tunnel Investigation at High Reynolds Numbers of Two Symmetrical Circular-Arc Airfoil Sections with High-Lift Devices. NACA RM No. L6K22, 1947.

5. Gustafson, F. B., and O'Sullivan, William J., Jr.: The Effect of High Wing Loading on Landing Technique and Distance, with Experimental Data for the B-26 Airplane. NACA ARR No. L4K07, 1945.

TABLE I

FUSELAGE ORDINATES

[Dimensions in inches]

Distance behind fuselage nose	Fuselage diameter
0	0.20
18.00	9.84
22.05	11.80
27.39	13.80
34.56	15.60
42.35	16.60
48.00	16.80
112.00	16.80
122.00	16.32
132.00	14.90
142.00	12.52
151.20	9.46
162.00	4.78
170.95	0

TABLE II

SUMMARY OF THE CHARACTERISTICS OF A CIRCULAR-ARC 42° SWEPTBACK WING WITH VARICUS FLAPS

Flap	$C_{L_{max}}$	$\alpha_{C_{L_{max}}}$ (deg)	D/L at 0.85 $C_{L_{max}}$	C_m curve	Figure no.
a. Wing					
None	0.85	20.0	0.208	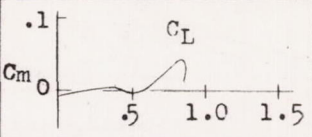	8
Split	.95	14.0	.193	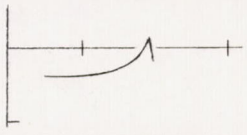	9
Flat leading edge	1.19	24.4	.190		8
Flat leading edge and split	1.53	21.5	.216	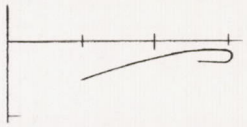	9
b. Wing-fuselage combination; midwing position					
None	0.89	20.0	0.226	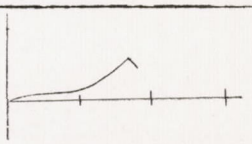	12
Split (cut-out)	1.00	17.0	.226	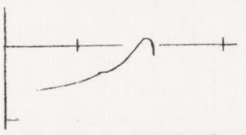	13
Flat leading edge	1.40	24.5	.202	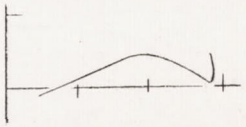	14
Flat leading edge and split	1.50	21.5	.190	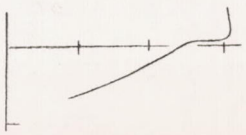	14

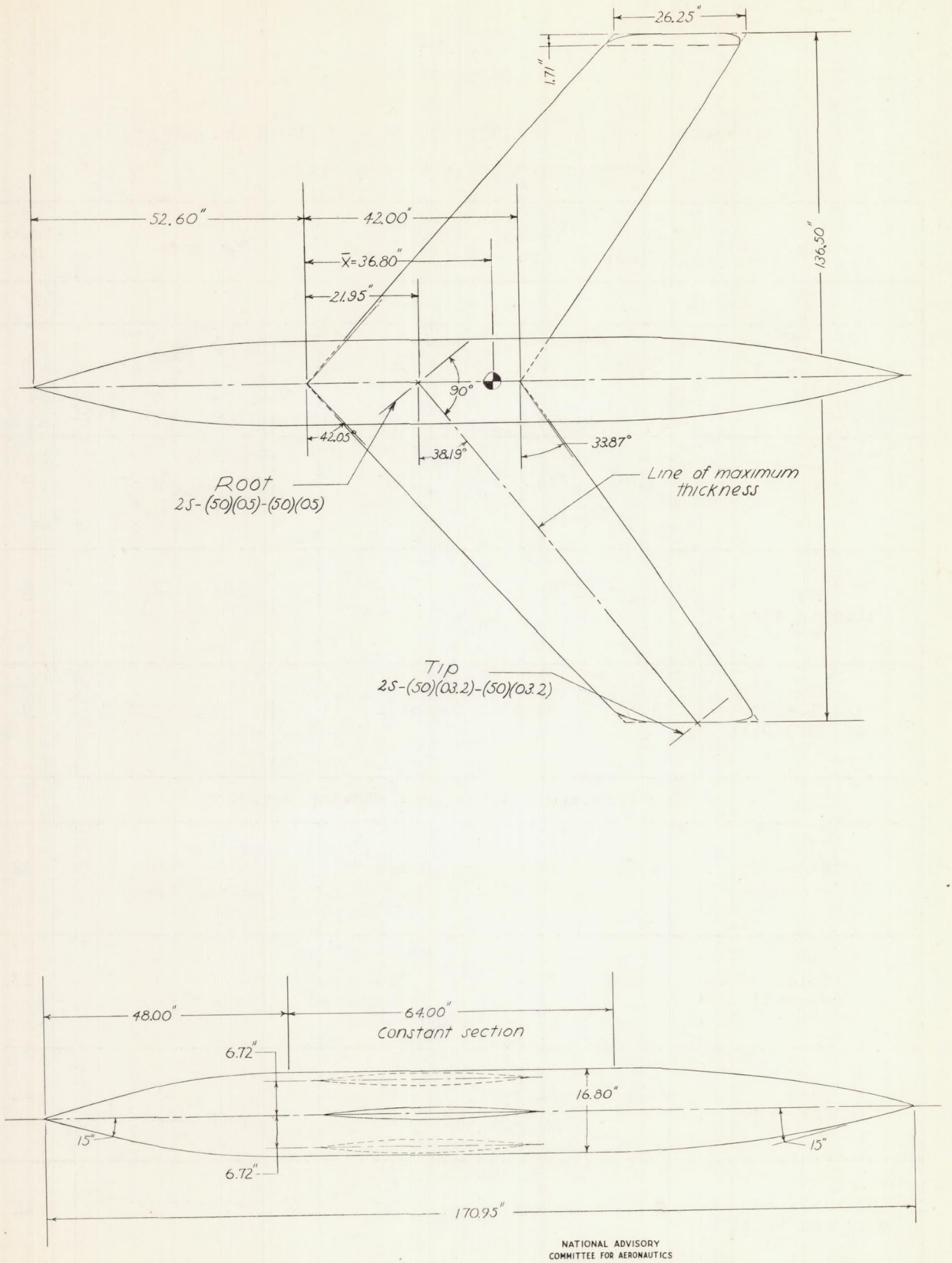

Figure 1.- Sketch of wing and fuselage. Wing area, 4728 sq.in.; mean aerodynamic chord, 35.31 in.; aspect ratio, 3.94.

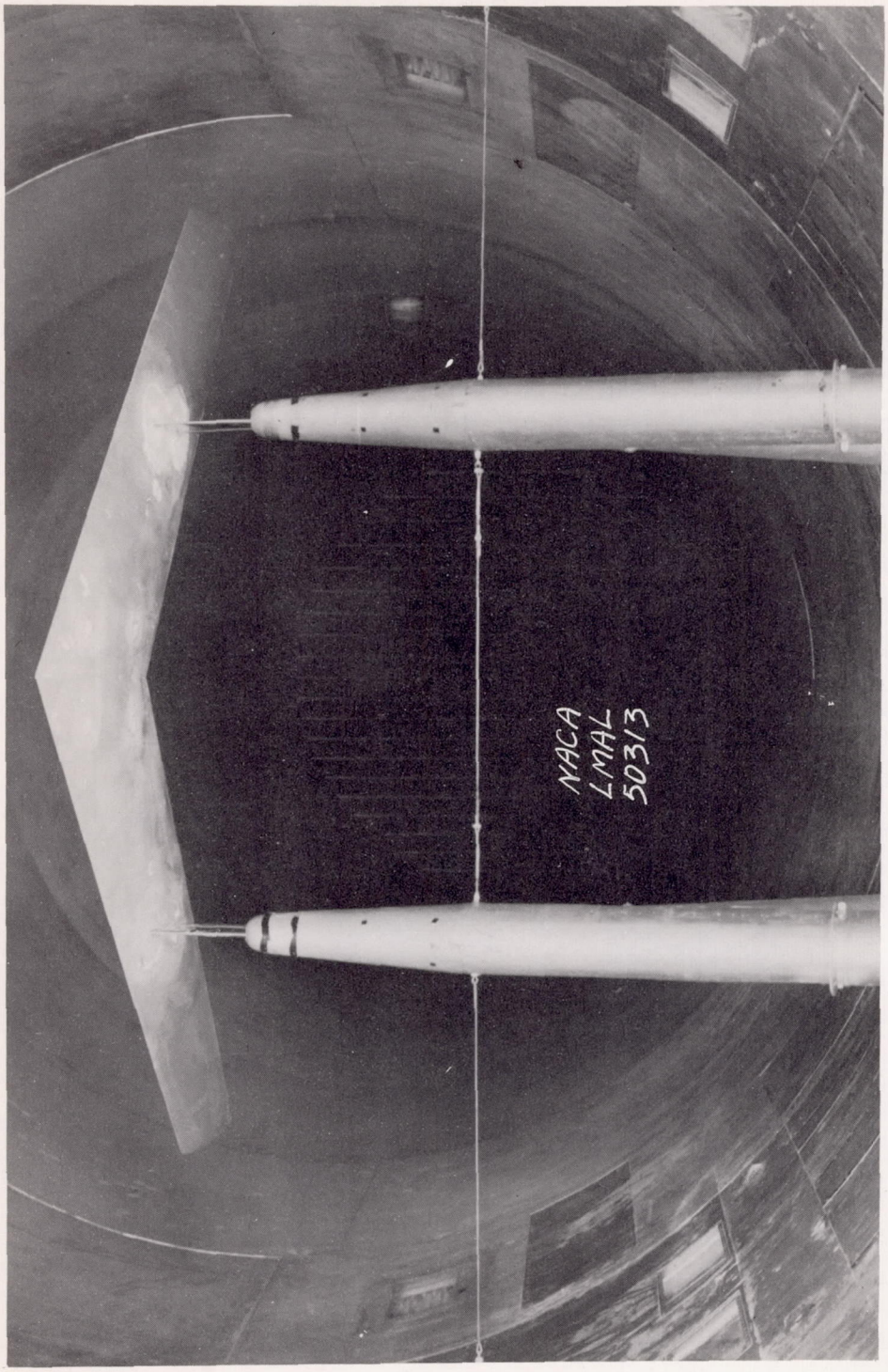

Figure 2.- A 42° sweptback wing mounted in the Langley 19-foot pressure tunnel.

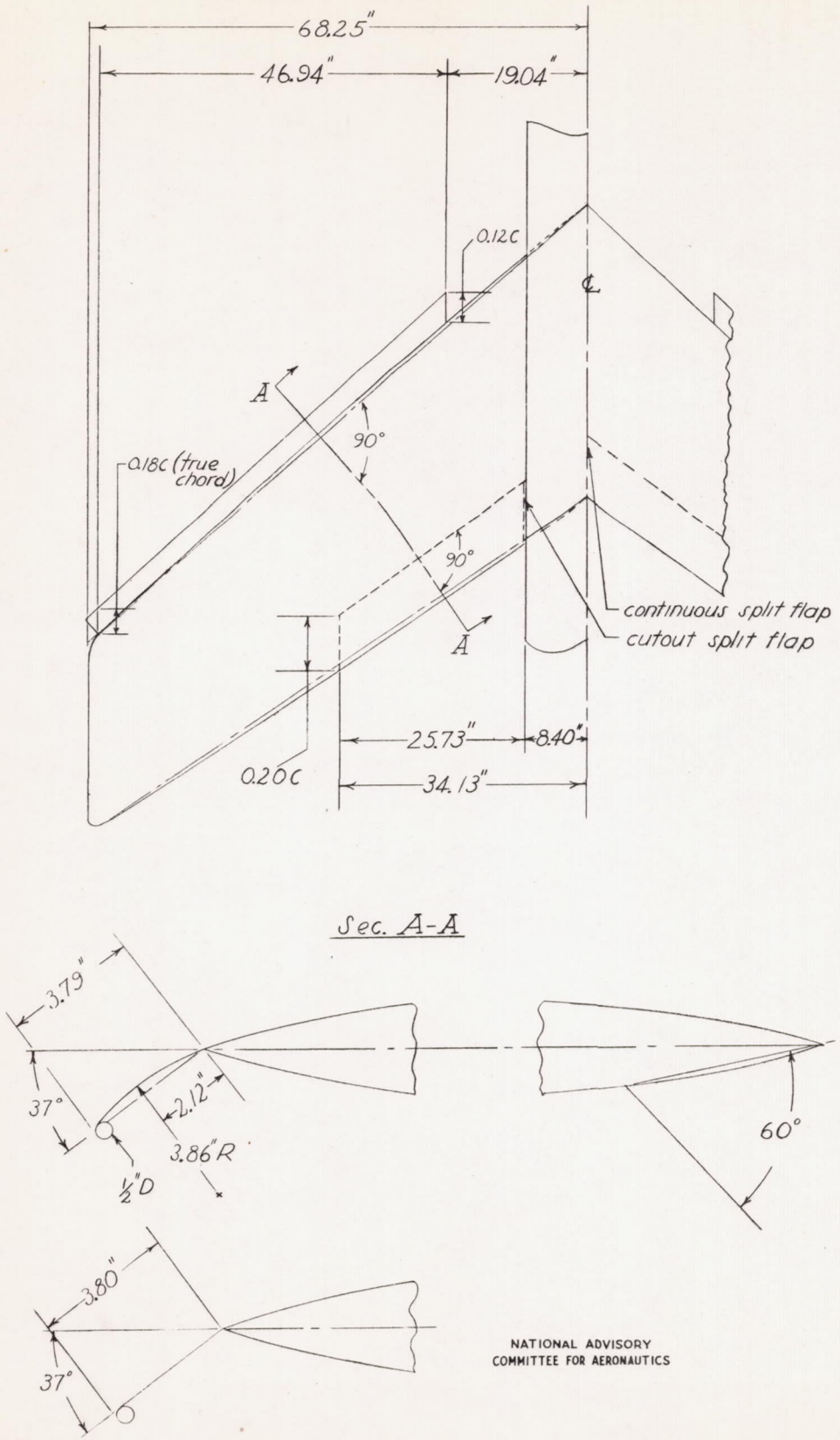

Figure 3 .- Schematic drawing of high lift devices for 42° swept-back wing.

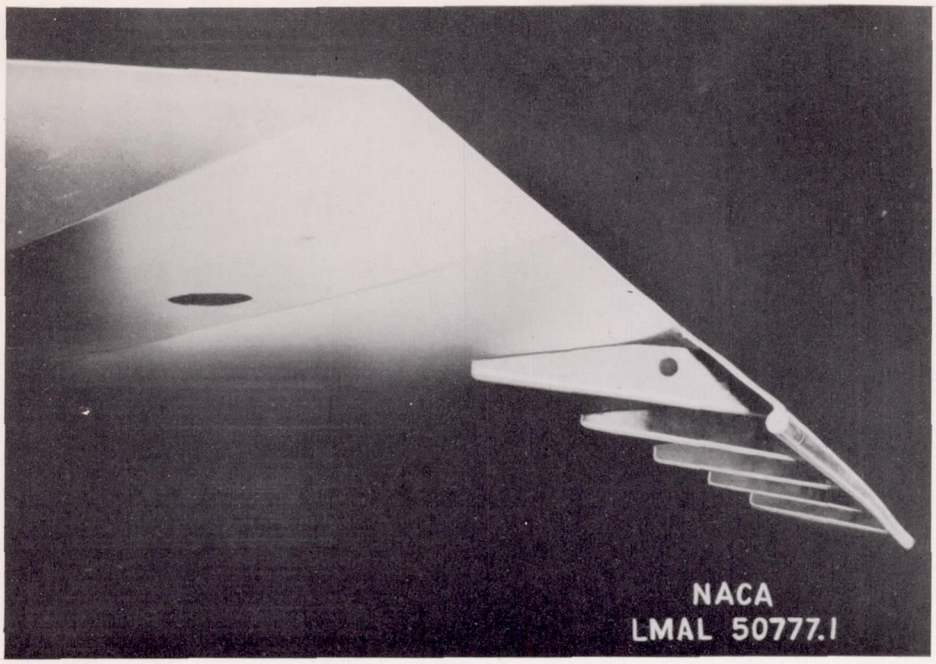

(a) Flat leading-edge flap.

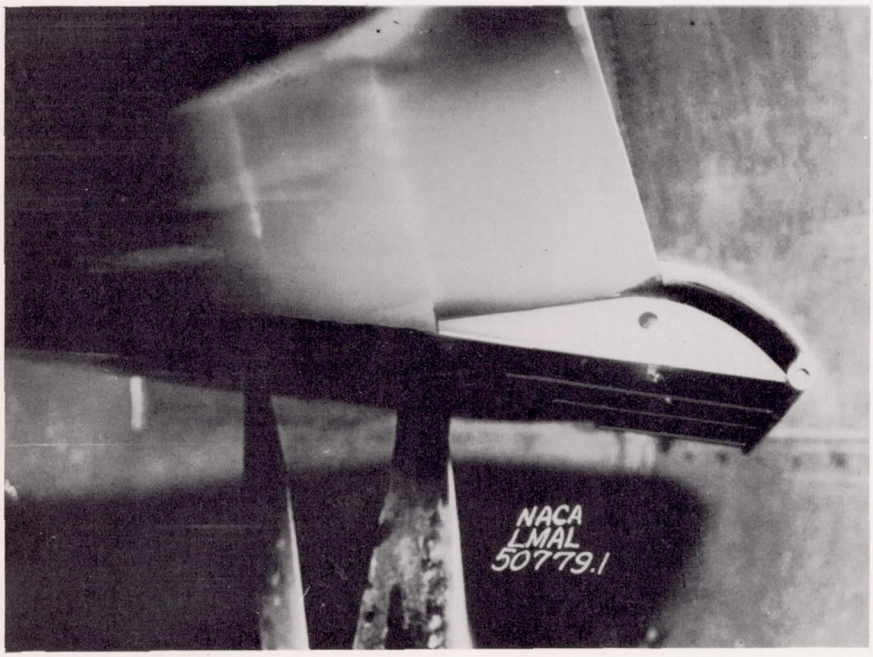

(b) Curved leading-edge flap.

Figure 4.- Leading-edge flap installation on 42° sweptback wing.

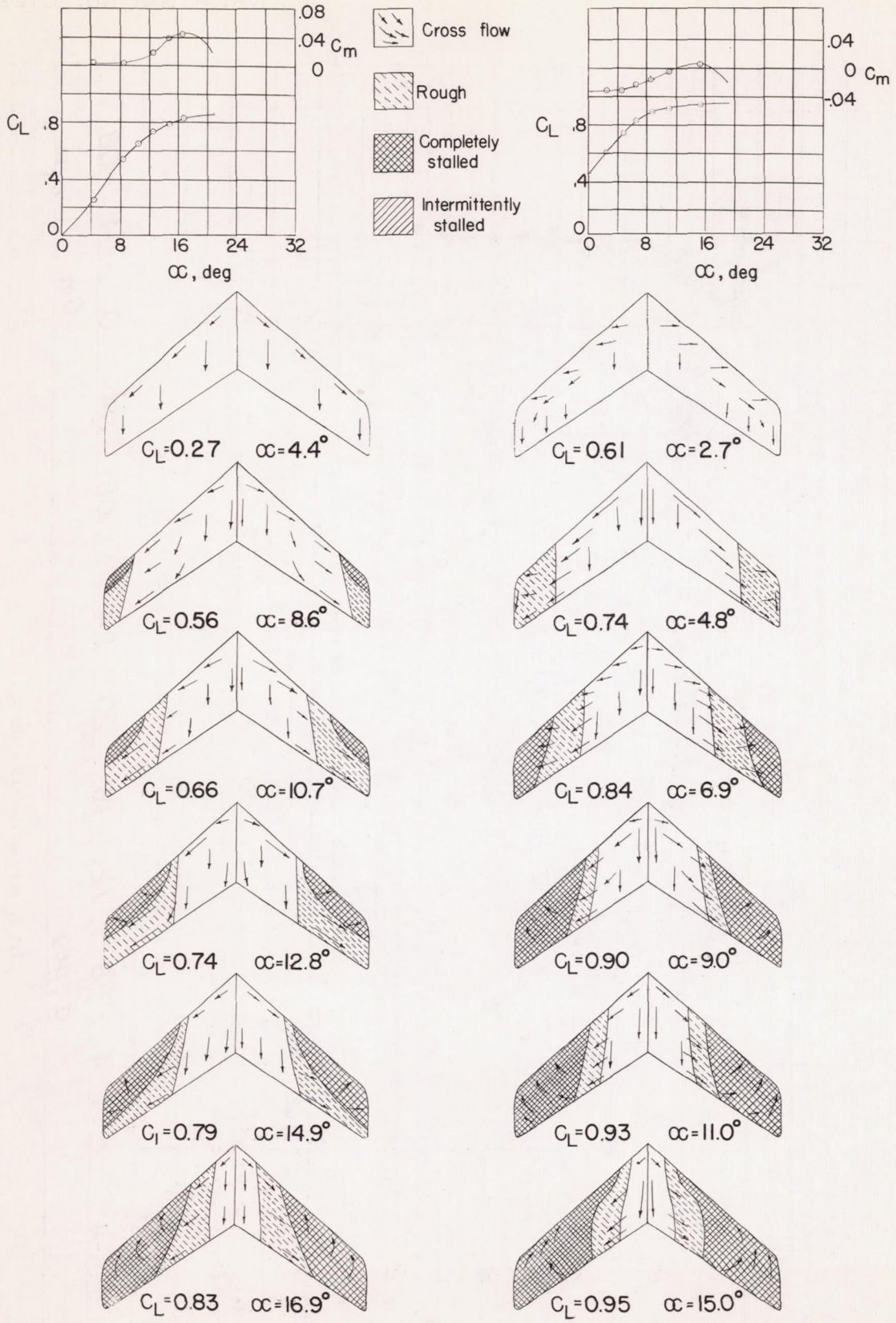

(a) Split flaps off. (b) Split flaps on.

NATIONAL ADVISORY COMMITTEE FOR AERONAUTICS

Figure 5 .- Stalling characteristics of a 42° sweptback wing. $R = 8.20 \times 10^6$.

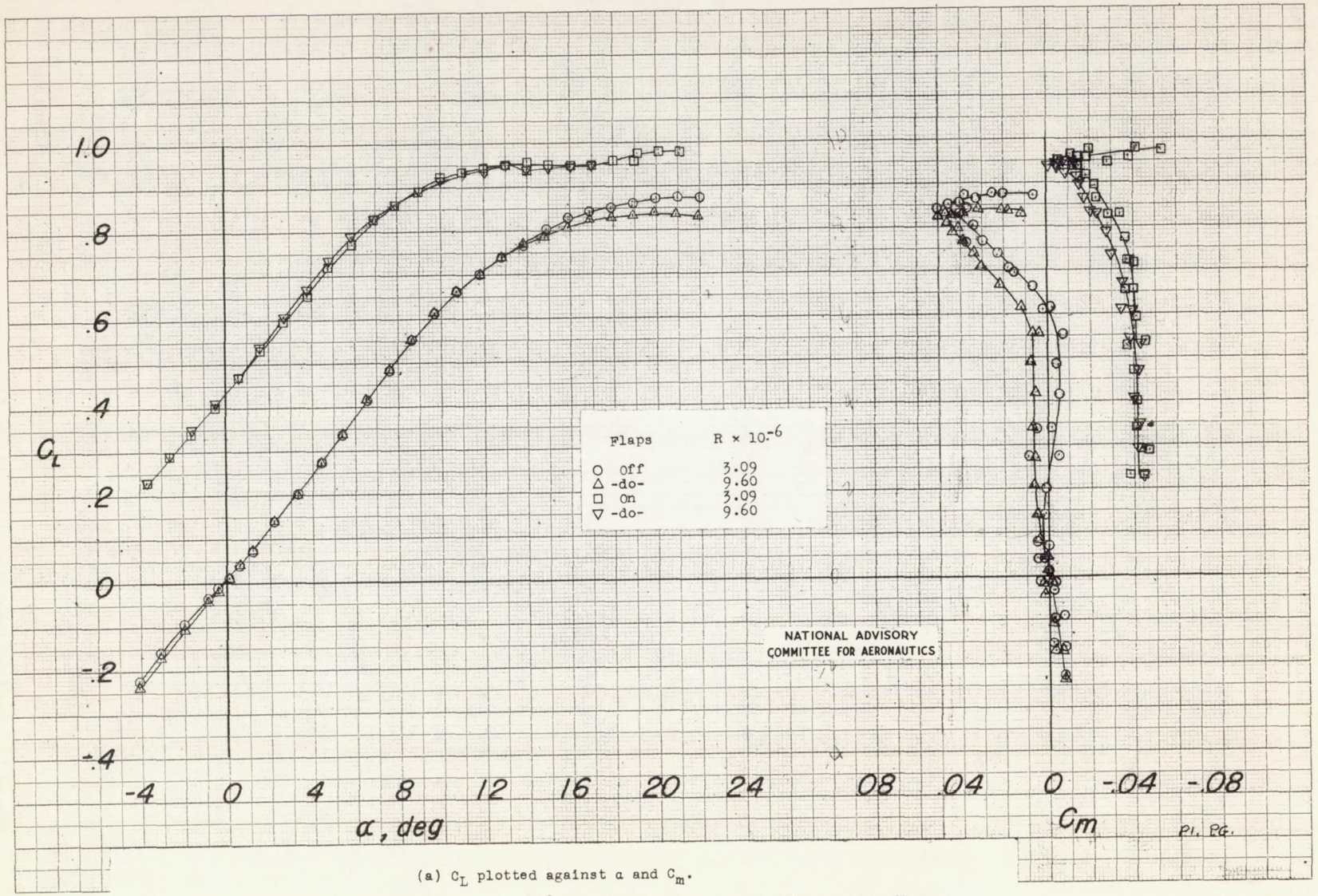

(a) C_L plotted against α and C_m.

Figure 6 .- Aerodynamic characteristics of a 42° sweptback wing with and without split flaps.

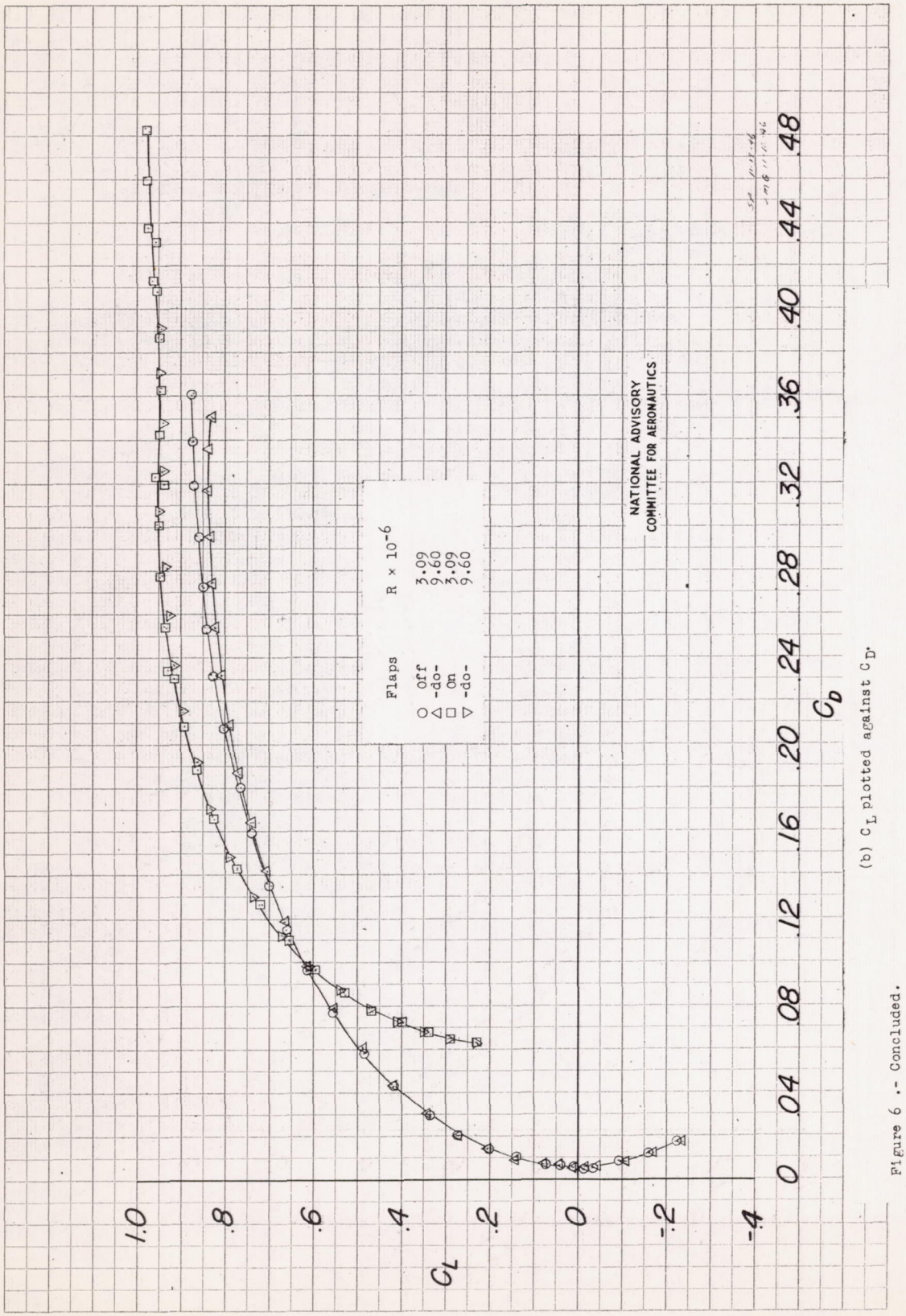

(b) C_L plotted against C_D.

Figure 6 .- Concluded.

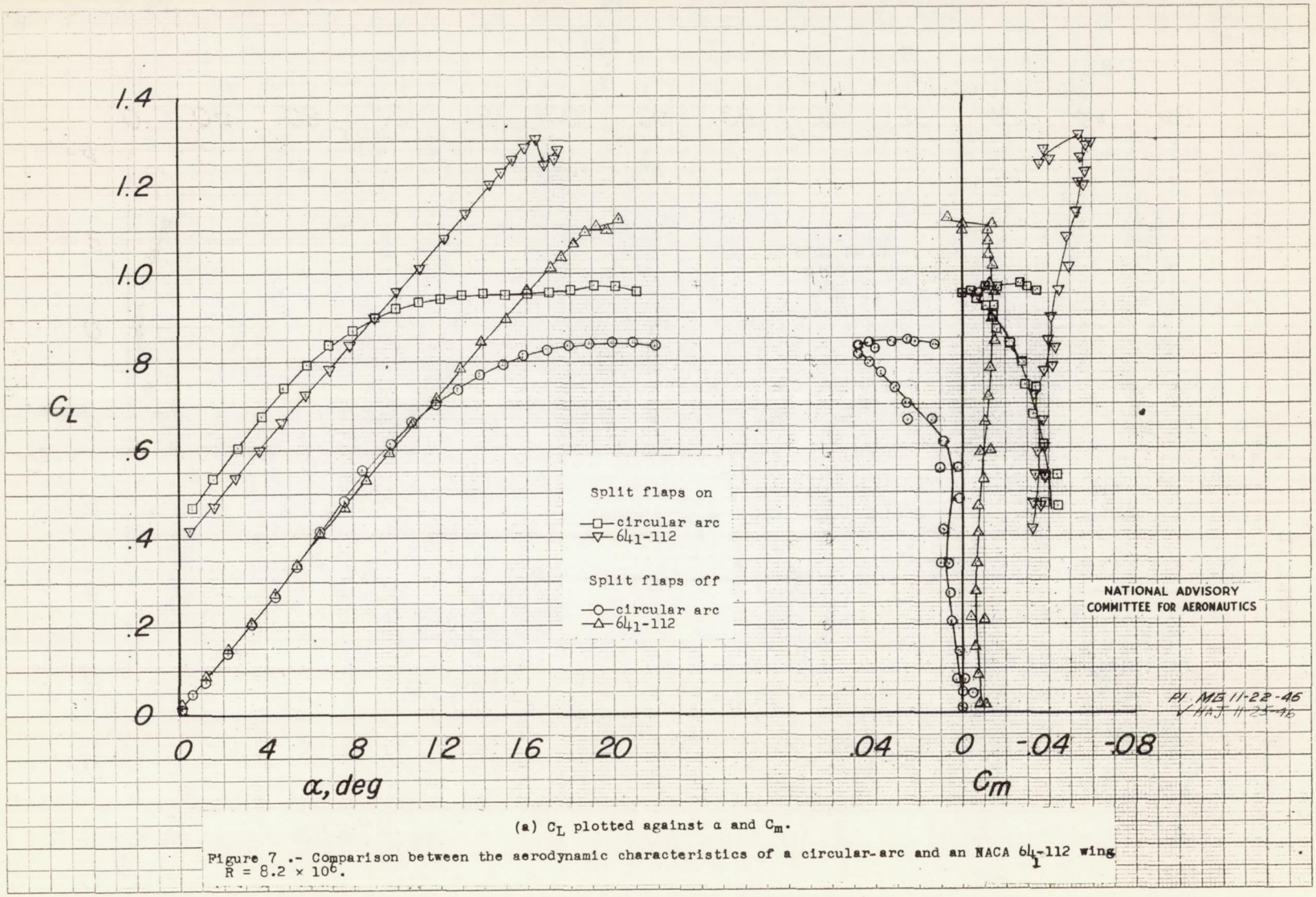

(a) C_L plotted against α and C_m.

Figure 7 .- Comparison between the aerodynamic characteristics of a circular-arc and an NACA 64_1-112 wing. $R = 8.2 \times 10^6$.

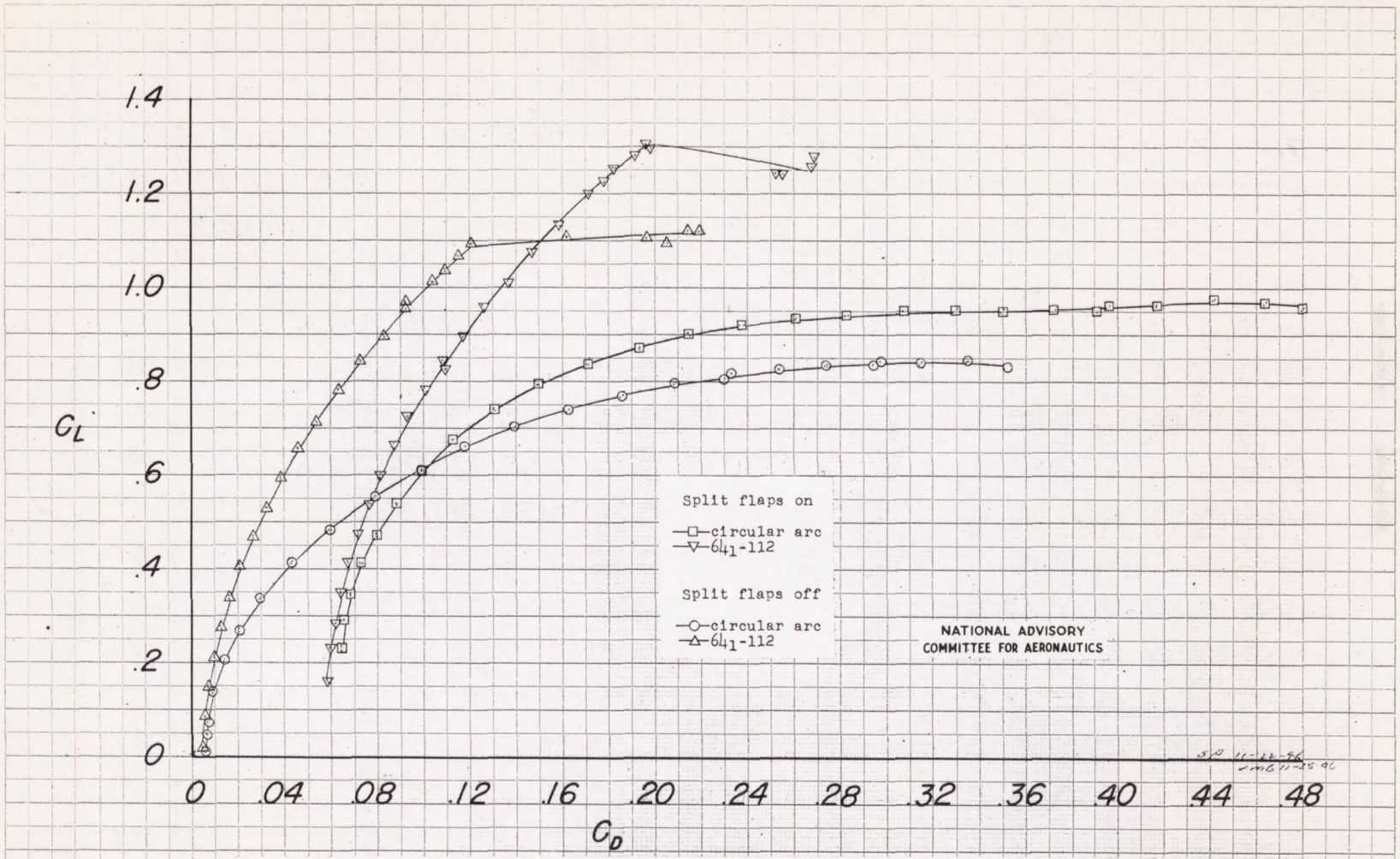

(b) C_L plotted against C_D.

Figure 7 .- Concluded.

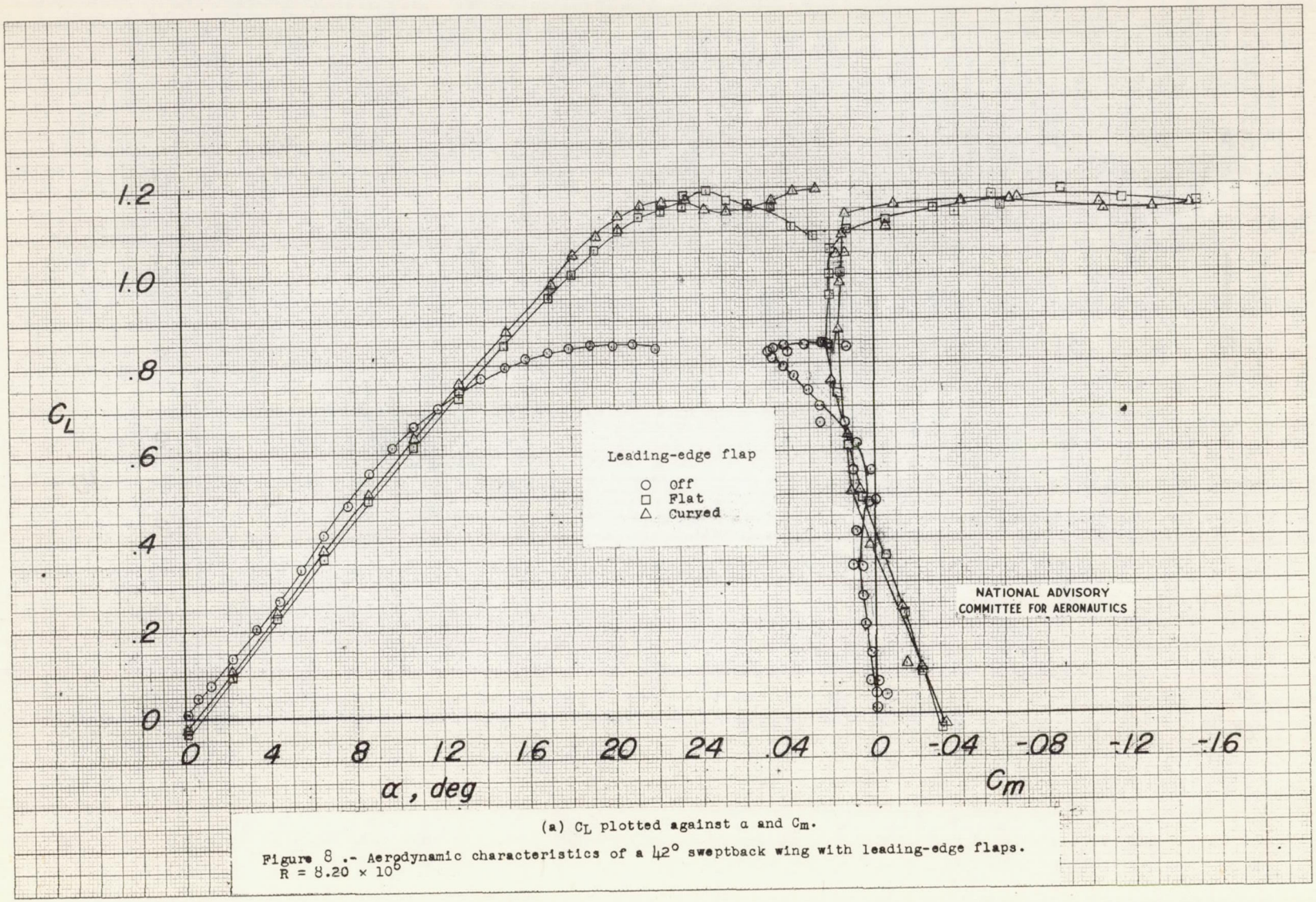

(a) C_L plotted against α and C_m.

Figure 8 .- Aerodynamic characteristics of a 42° sweptback wing with leading-edge flaps.
$R = 8.20 \times 10^6$

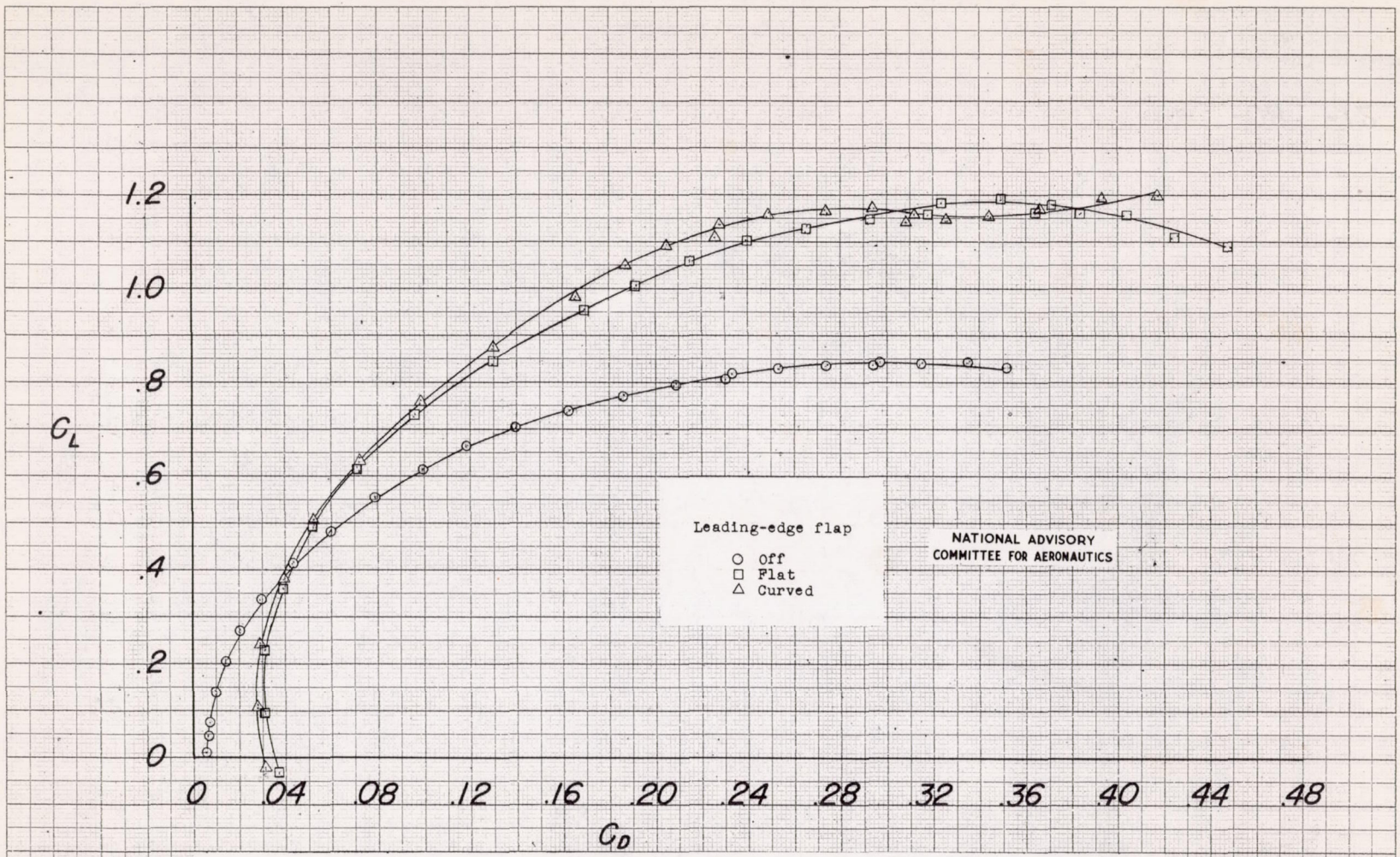

(b) C_L plotted against C_D.

Figure 8 .- Concluded.

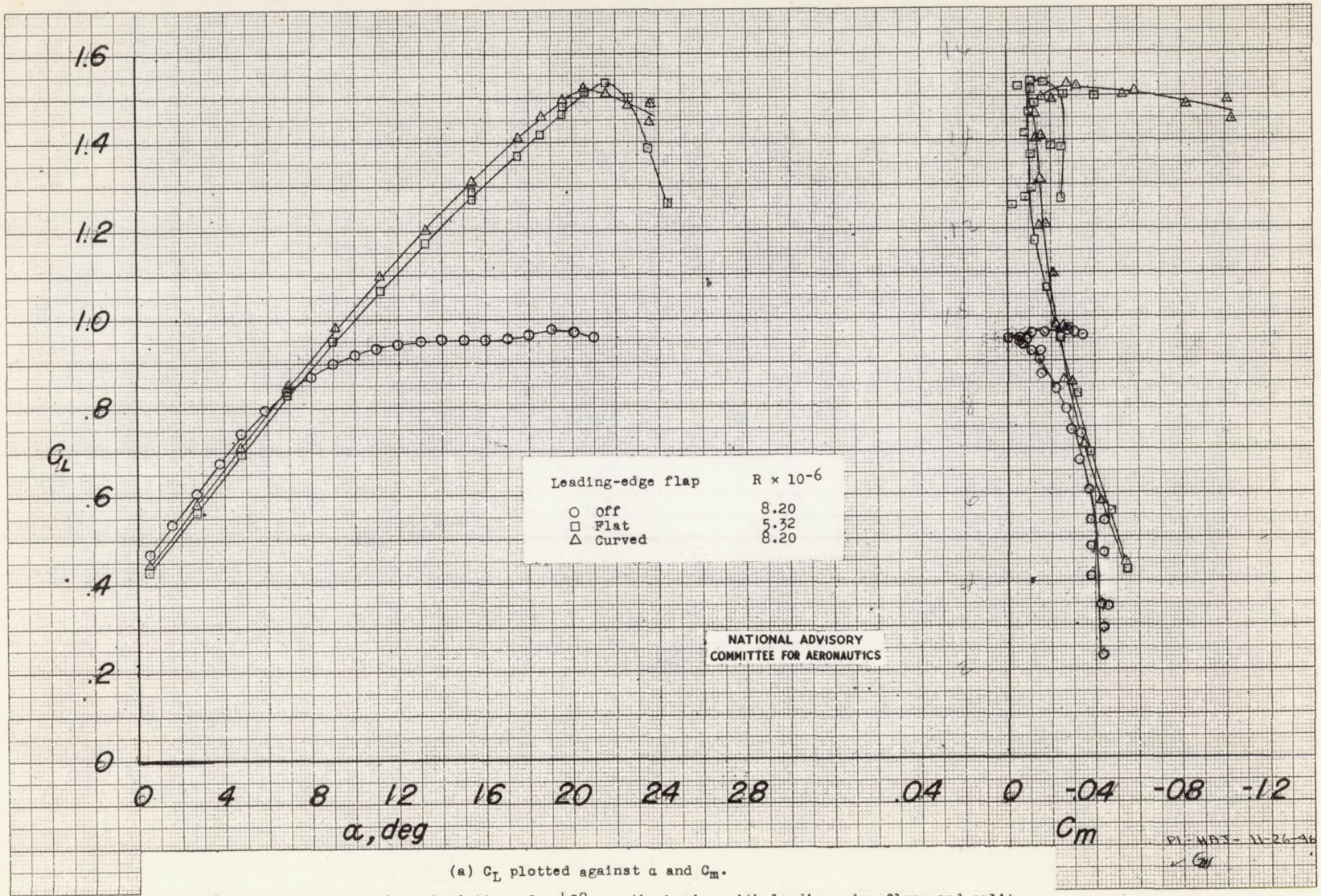

(a) C_L plotted against α and C_m.

Figure 9 .- Aerodynamic characteristics of a 42° sweptback wing with leading-edge flaps and split flaps.

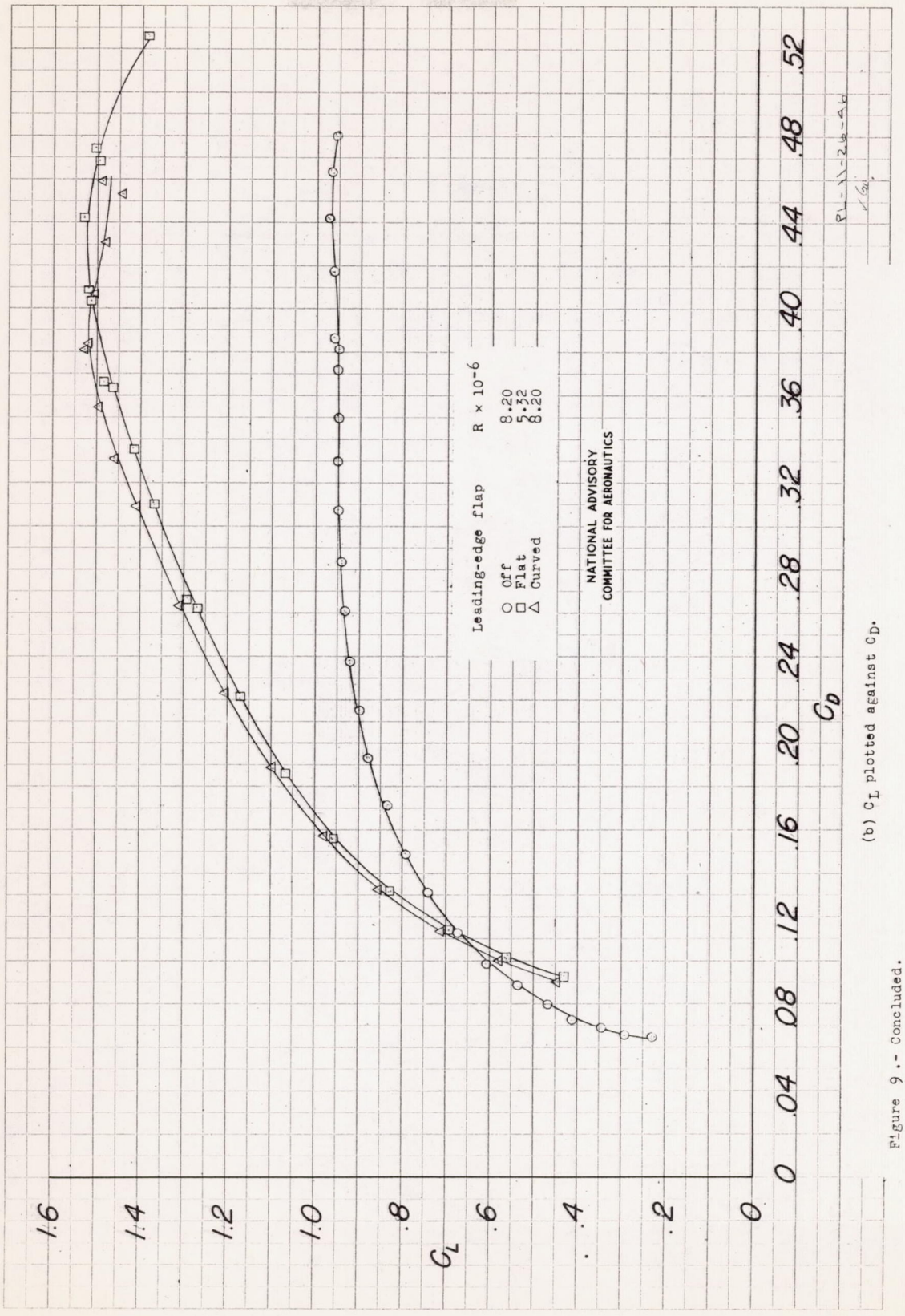

(b) C_L plotted against C_D.

Figure 9.- Concluded.

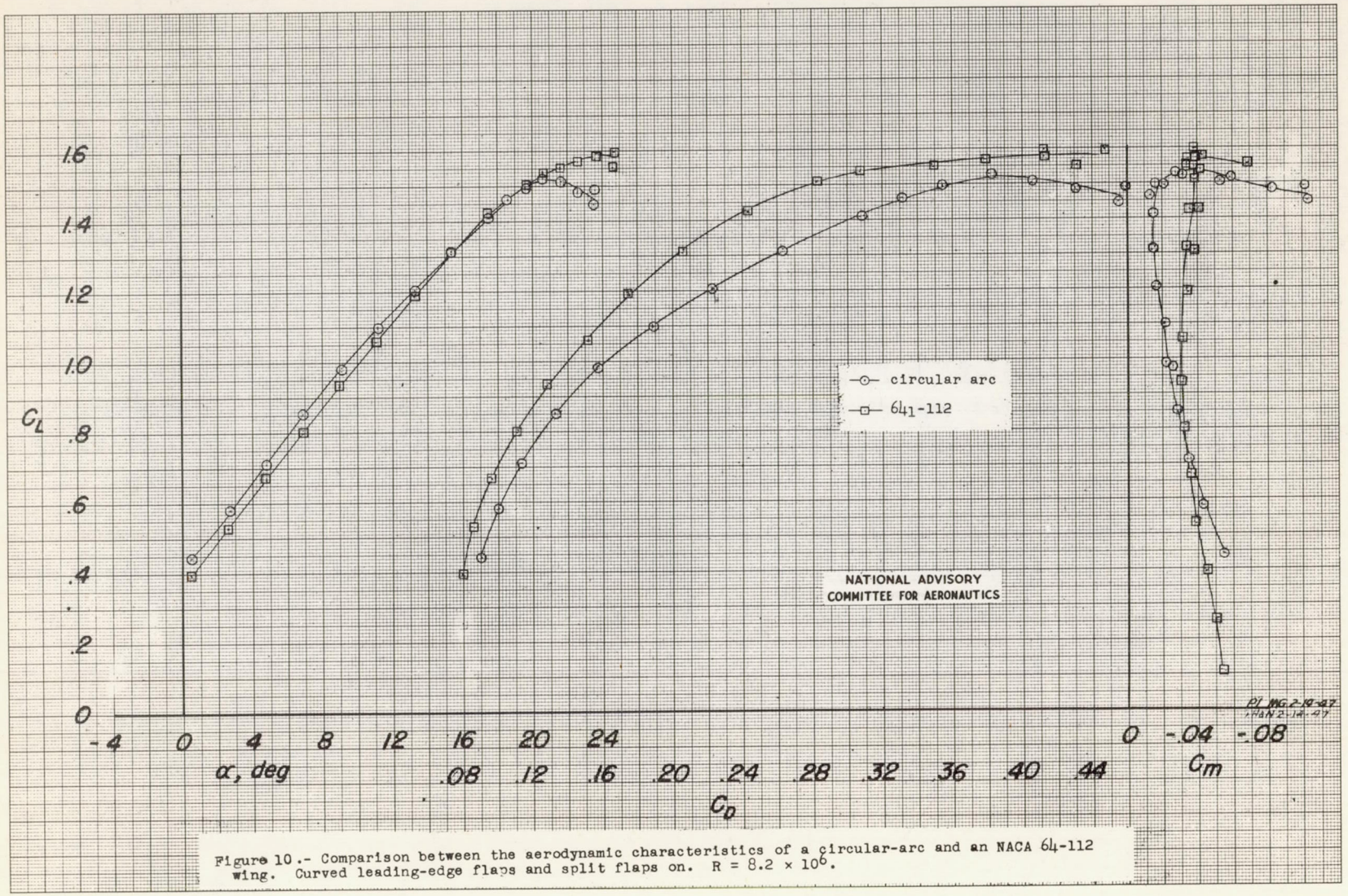

Figure 10.- Comparison between the aerodynamic characteristics of a circular-arc and an NACA 64-112 wing. Curved leading-edge flaps and split flaps on. $R = 8.2 \times 10^6$.

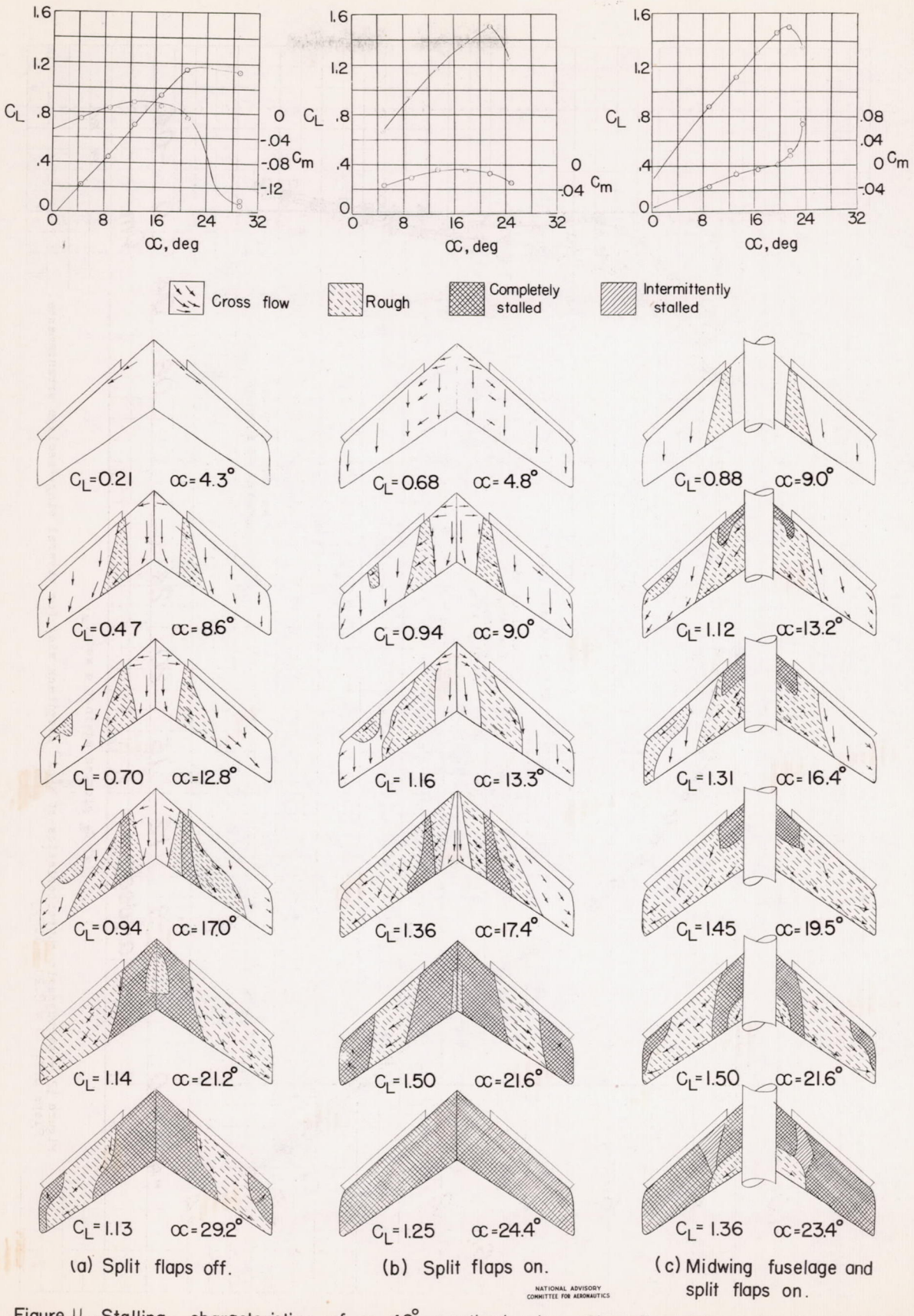

(a) Split flaps off. (b) Split flaps on. (c) Midwing fuselage and split flaps on.

NATIONAL ADVISORY COMMITTEE FOR AERONAUTICS

Figure 11.-Stalling characteristics of a 42° sweptback wing with a flat leading-edge flap $R=5.32 \times 10^6$.

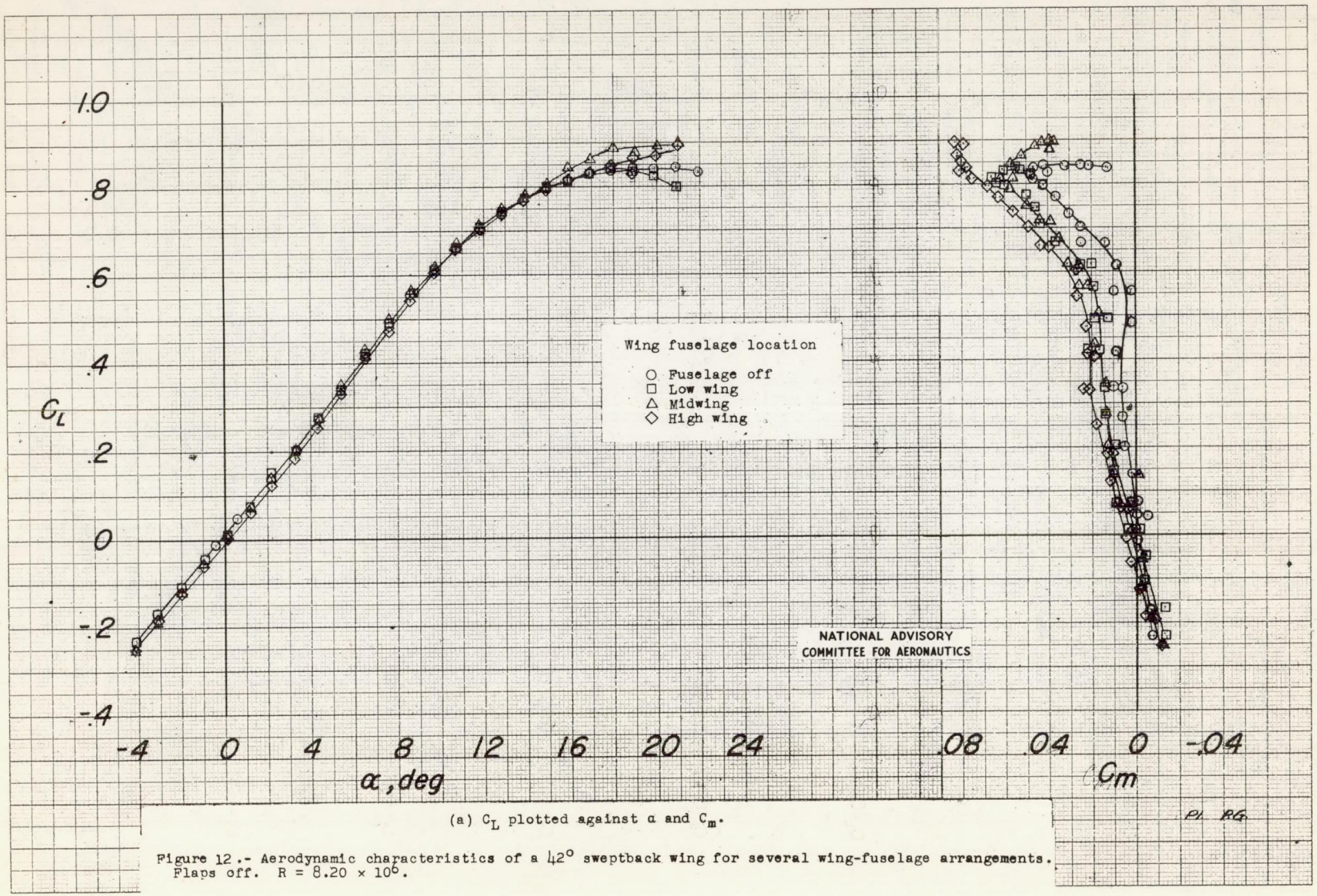

(a) C_L plotted against α and C_m.

Figure 12.- Aerodynamic characteristics of a 42° sweptback wing for several wing-fuselage arrangements. Flaps off. $R = 8.20 \times 10^6$.

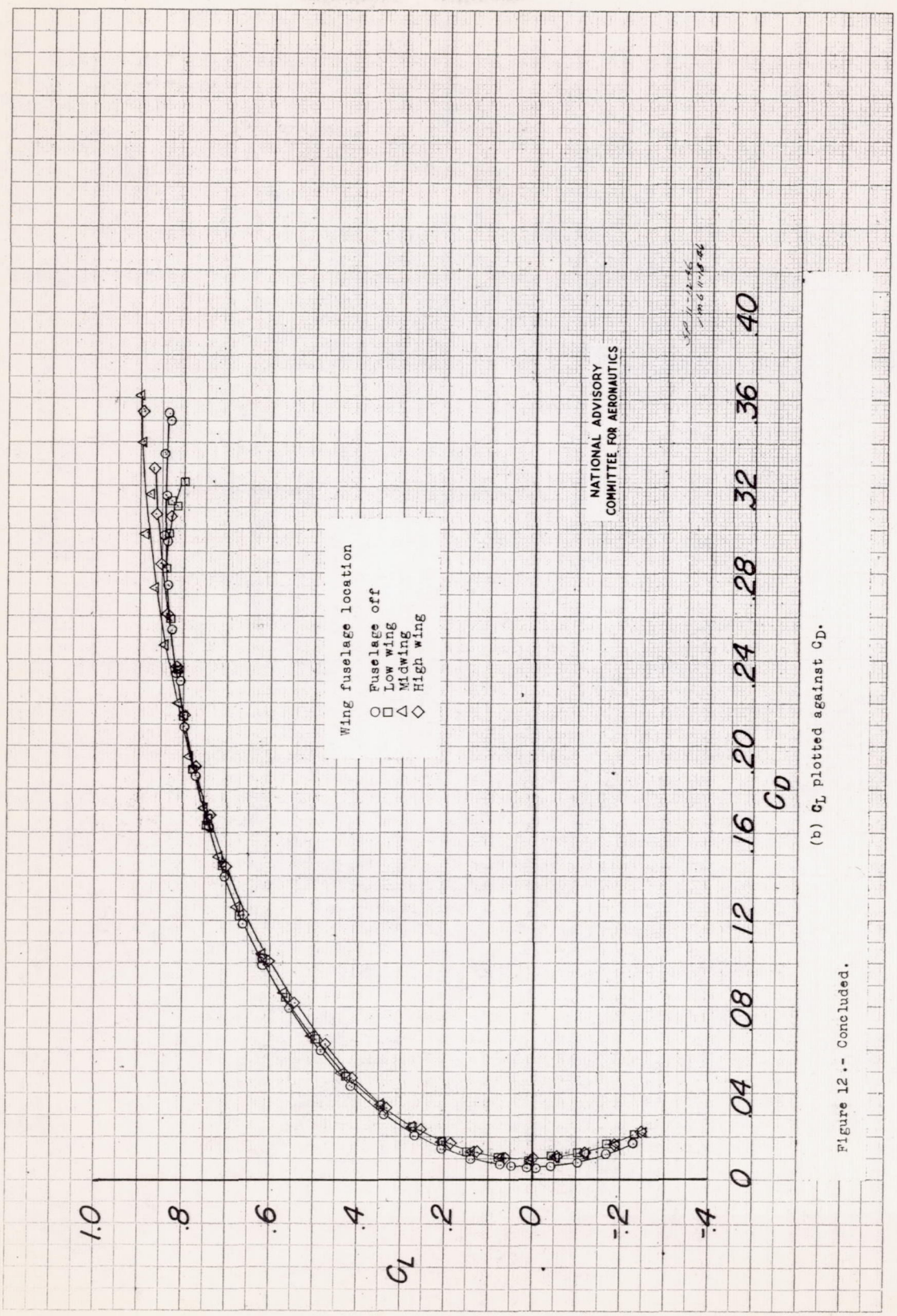

(b) C_L plotted against C_D.

Figure 12.- Concluded.

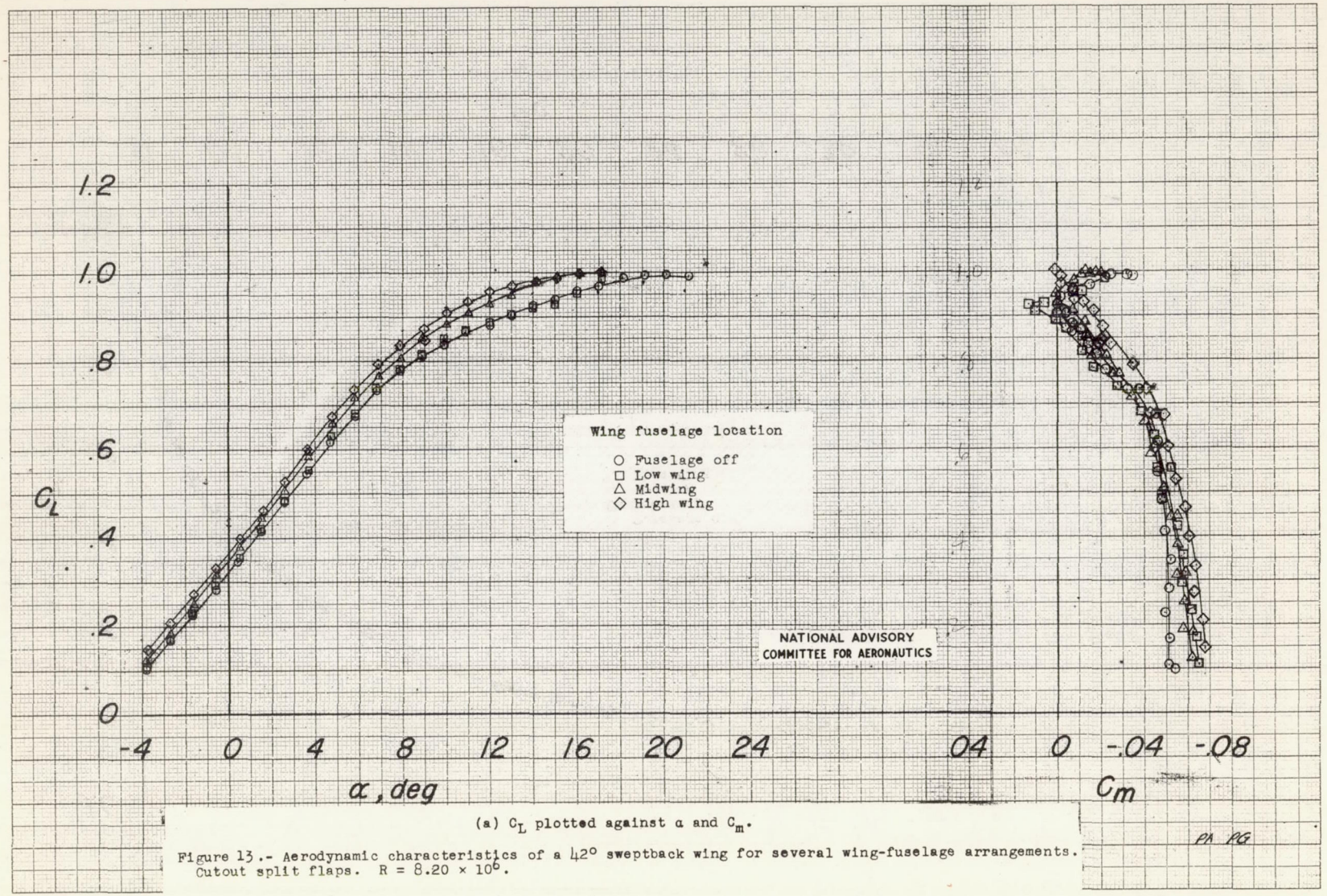

(a) C_L plotted against α and C_m.

Figure 13.- Aerodynamic characteristics of a 42° sweptback wing for several wing-fuselage arrangements. Cutout split flaps. $R = 8.20 \times 10^6$.

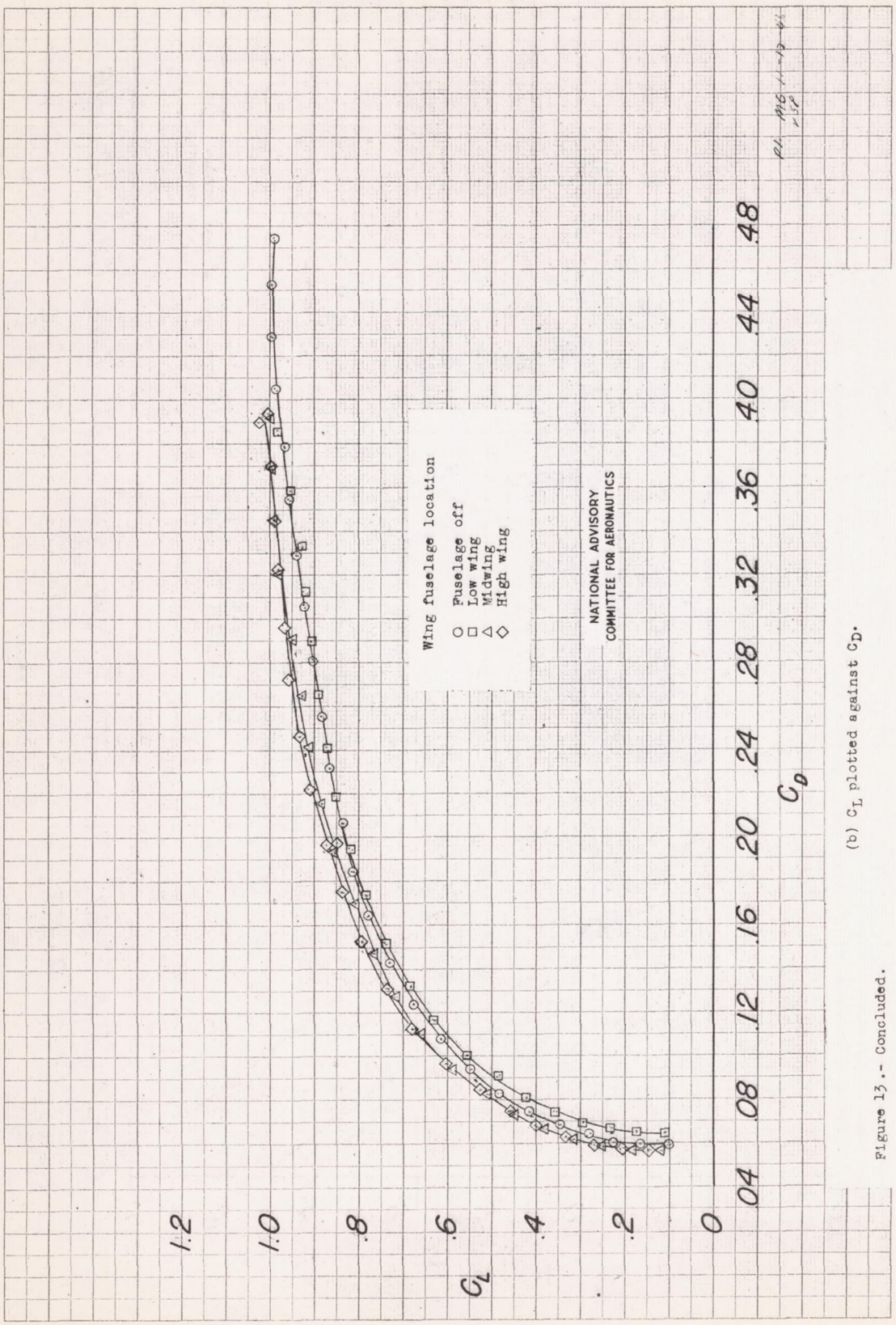

(b) C_L plotted against C_D.

Figure 13.- Concluded.

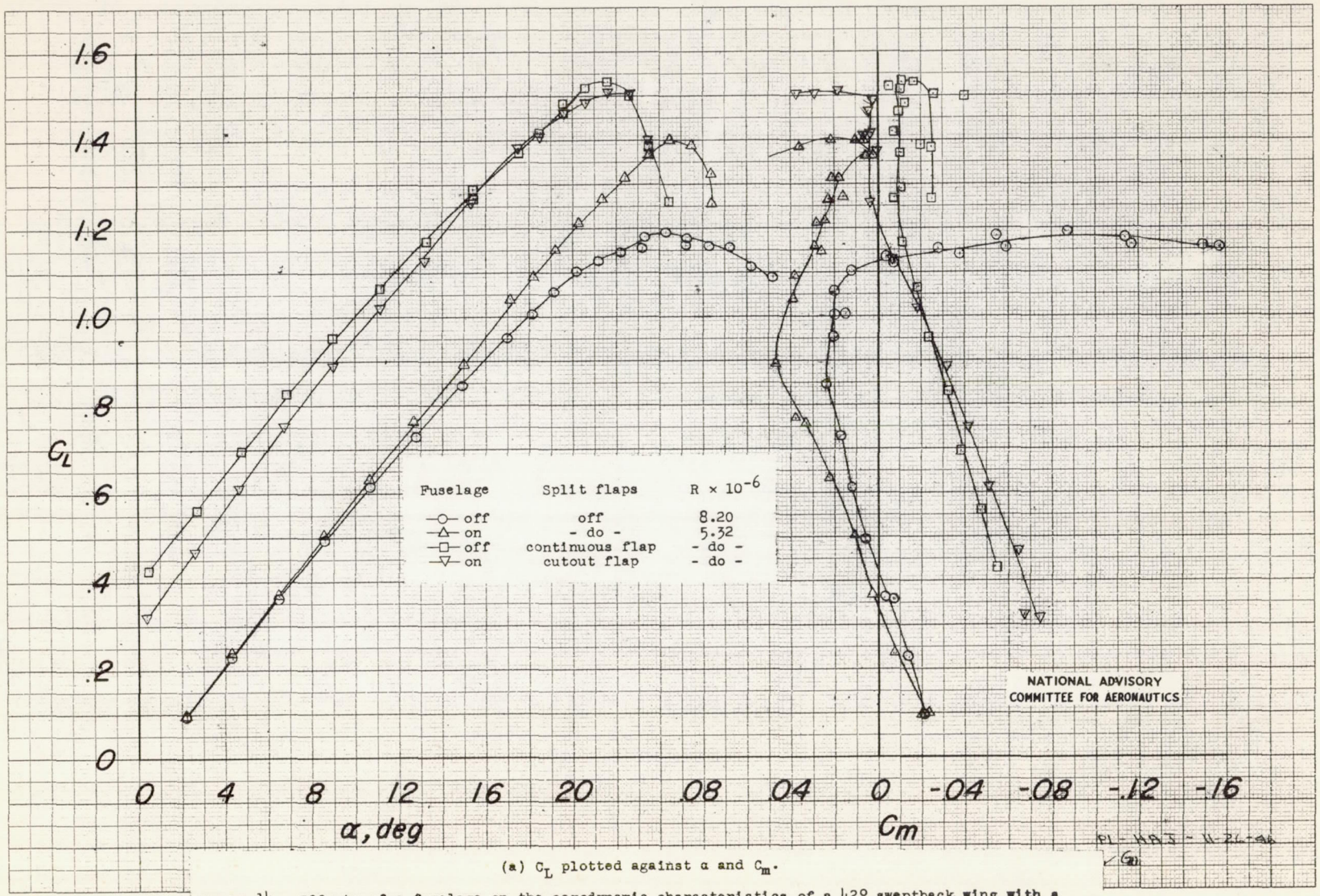

(a) C_L plotted against α and C_m.

Figure 14.- Effects of a fuselage on the aerodynamic characteristics of a 42° sweptback wing with a flat leading-edge flap. Midwing position.

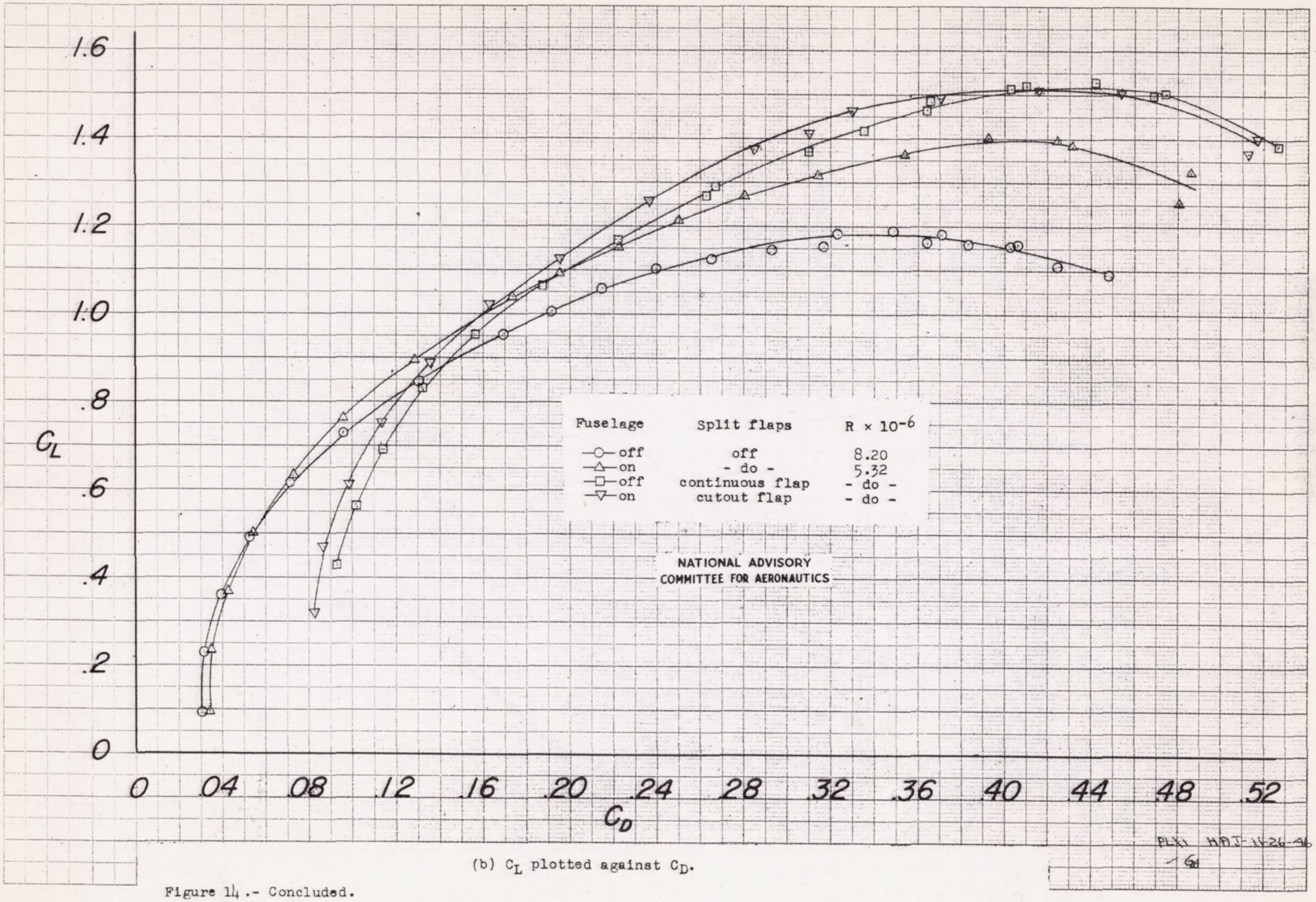

(b) C_L plotted against C_D.

Figure 14.- Concluded.

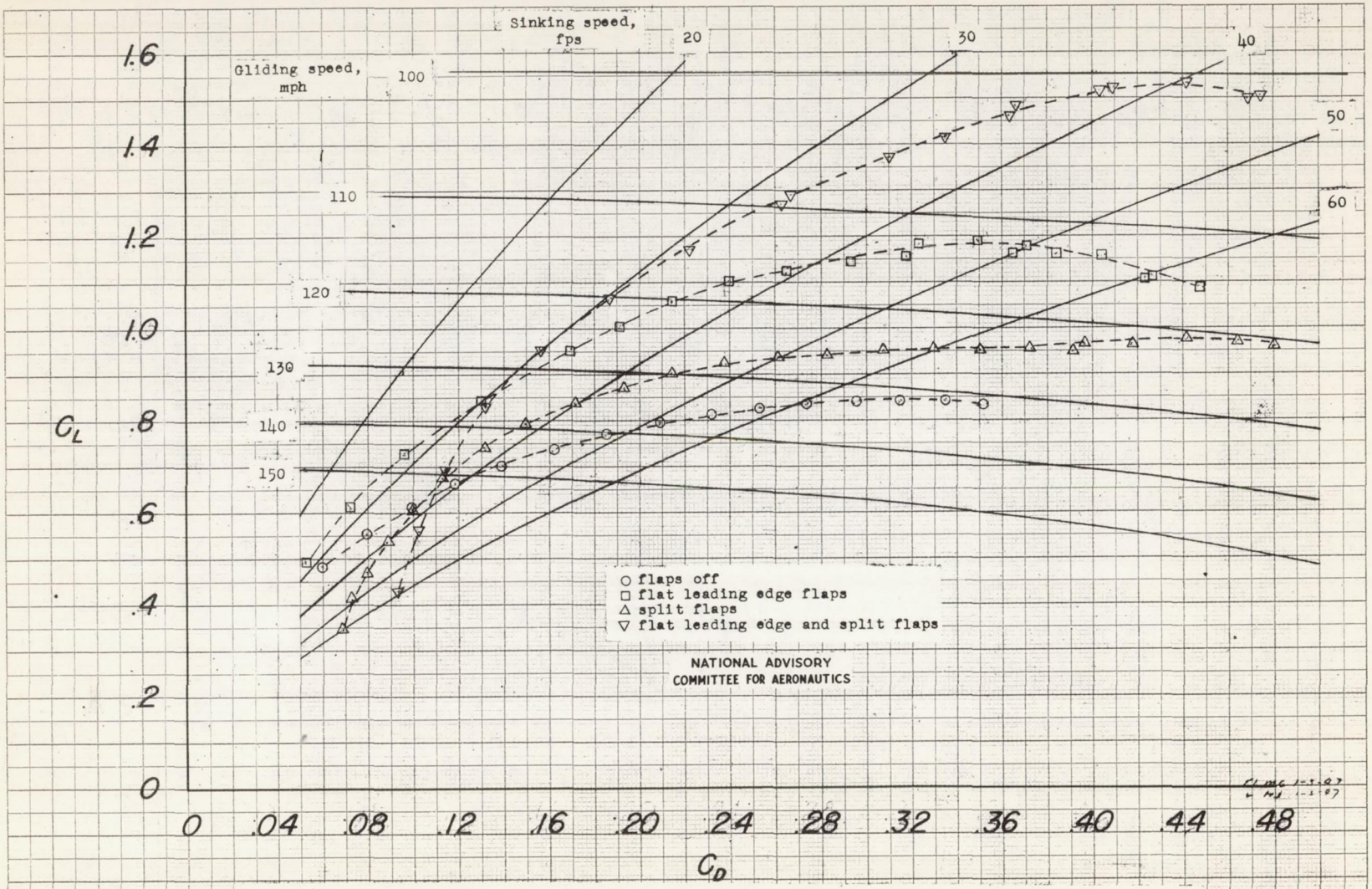

Figure 15 - Glide characteristics of a 42° sweptback wing for a wing loading of 40 pounds per square foot.

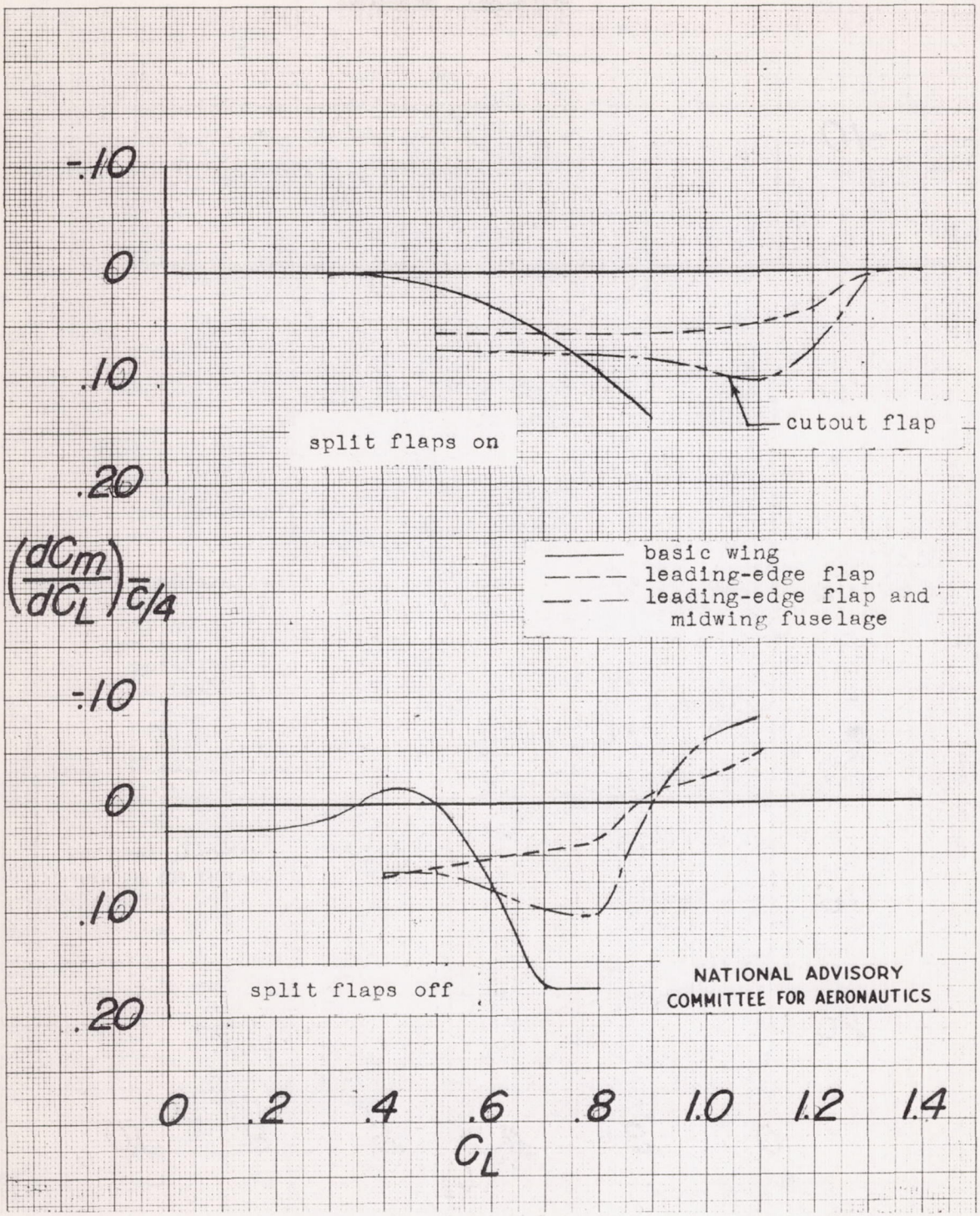

Figure 16.- Variation of $(dC_m/dC_L)_{\bar{c}/4}$ with lift coefficient for a 42° sweptback wing with and without a flat leading-edge flap. $R = 5.32 \times 10^6$.

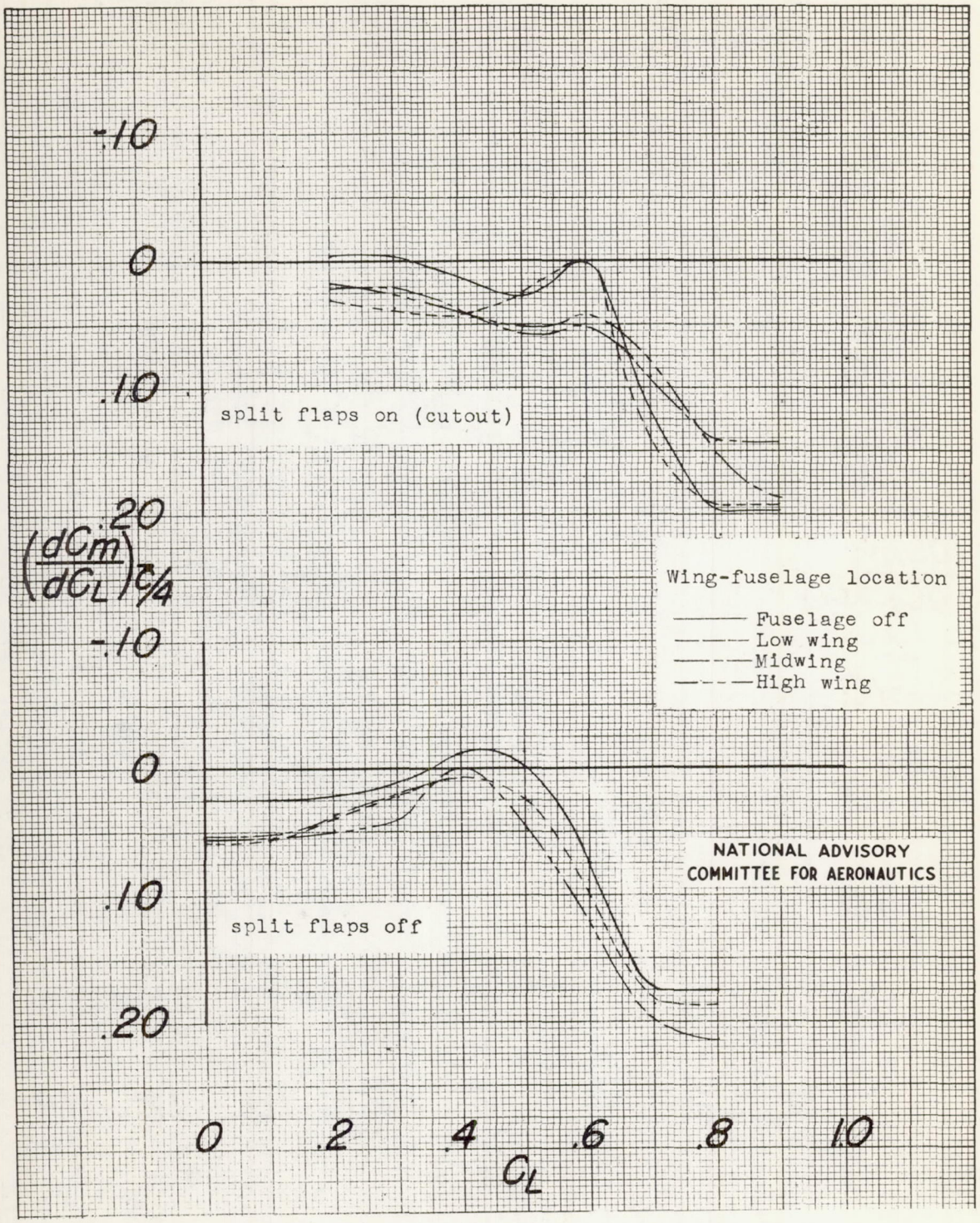

Figure 17.- Variation of $(dC_m/dC_L)_{\bar{c}/4}$ with lift coefficient for a 42° swept-back wing for several wing-fuselage arrangements. $R = 8.2 \times 10^6$.